2

Transistor Properties Applicable to Oscillator Design

2.1 INTRODUCTION

This chapter presents a brief review of transistor models suitable for oscillator design and describes the approximations and simplifications necessary to render the models amenable to relatively simple mathematical manipulation. In doing so, full advantage is taken of the present availability of high-performance low-cost transistors which incidently also help to simplify the application theory.

The models are very correct at low frequency of operation. As the frequency increases, they become less and less accurate until they become almost useless.

An additional major operating parameter which strongly influences the accuracy of the models is the emitter dc current, I_E. Again, as the current increases, the accuracy of the models decreases.

In order to ensure that the transistor characteristics are such as to result in good accuracy of the oscillator circuit algorithms, the input data for each algorithm includes a relationship between the f_T, f, and some direct function of I_E. If this relationship is satisfied, the algorithm will be reasonably accurate.

It is almost impossible to develop a satisfactory transistor model with fixed parameters or parameters that vary in a simple fashion with frequency over a wide frequency range, particularly at high frequencies. At the large signals which exist in real oscillators, the problem is rendered much more difficult.

2.2 TWO-PORT SMALL-SIGNAL TRANSISTOR MODELS

The two-port network theory stated in Section 1.2.2 applies equally well to transistors at small-signal levels. This theory results in transistor parameters

which, because they are only for small signals, are useful in determining whether the oscillator small-signal gain is sufficiently large to start oscillations in a given oscillator configuration. However, that is not a trivial achievement and for that reason, the small-signal theory is presented. The small-signal theory will also serve as a starting point for the large-signal theory.

As pointed out in Section 1.2.2, network models can be developed for transistors operating at large-signal levels but the mathematical operations using these models are very limited.

The usual transistor has three terminals and one of these terminals can be considered a common terminal, as shown in Fig. 2.1. The transistors shown are bipolar but they can just as well be FET's, in which case *gate* is substituted for *base*, *drain* for *collector*, and *source* for *emitter*.

To indicate clearly that the device, within the box, is an active device, a different type of notation may be used. For example:

$$y_{11e} \text{ is written } y_{ie}$$

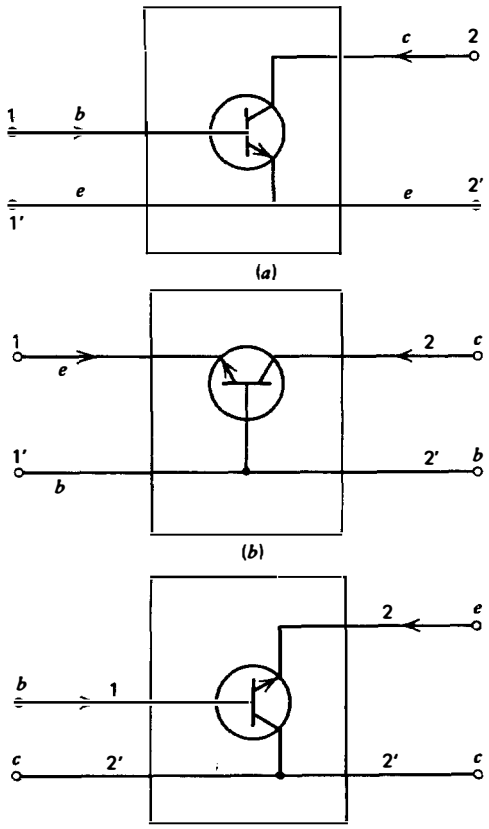

Figure 2.1 The three possible representations of a transistor as a two-port network. (*a*) Common emitter. (*b*) Common base. (*c*) Common collector.

where i signifies 11 and e indicates that the emitter is common. Similarly,

$$y_{fe} \text{ is equivalent to } y_{21e}$$

$$y_{re} \text{ is equivalent to } y_{12e}$$

$$y_{oe} \text{ is equivalent to } y_{22e}$$

where $i \equiv$ input, $f \equiv$ forward, $r \equiv$ reverse, and $o \equiv$ output. In this book, both forms of notation are used.

Three types of parameters have already been discussed in Section 1.2.2, the y, z, and h parameters. For transistors, an additional type of parameter, the s parameter, or scattering coefficients, is also used and is gradually becoming more and more popular. More transistor data are being presented in s parameter form. The advantage of the s parameter is that the measurements can be made easily since the terminations are always 50 Ω or some other medium impedance standard termination which has been highly developed over many years. The y parameters are short-circuit parameters; the z parameters are open-circuit parameters; and the h parameters are combination short- and open-circuit parameters. It is very difficult to obtain good open circuits, and shorts at high frequencies while 50-Ω accurate terminations are widely available and the s parameter measurements can be easily made with conventional network analyzers. Also, the transistor may oscillate with an open- or short-circuit termination.

The user of the transistor has to have the performance data available. Unfortunately, some manufacturers may supply the data in only one parameter type and one common element configuration. The user has to be able to transform this information into some other parameter type and other configuration. To perform this transformation, the relationships given below can be used. These relationships are in addition to those in Section 1.2.2.7.

2.2.1 Conversions among h, y, and z Parameters

2.2.1.1 h to y

$$y_{11} = \frac{1}{h_{11}}, \qquad y_{12} = \frac{-h_{12}}{h_{11}}, \qquad y_{21} = \frac{h_{21}}{h_{11}}, \qquad y_{22} = \frac{\Delta h}{h_{11}} \tag{2.1}$$

where $\Delta h = h_{11}h_{22} - h_{12}h_{21}$.

2.2.1.2 y to h

$$h_{11} = \frac{1}{y_{11}}, \qquad h_{12} = \frac{-y_{12}}{y_{11}}, \qquad h_{21} = \frac{y_{21}}{y_{11}}, \qquad h_{22} = \frac{\Delta y}{y_{11}} \tag{2.2}$$

where $\Delta y = y_{11}y_{22} - y_{12}y_{21}$.

2.2.1.3 *h to z*

$$z_{11} = \frac{\Delta h}{h_{22}}, \qquad z_{12} = \frac{h_{12}}{h_{22}}, \qquad z_{21} = \frac{-h_{21}}{h_{22}}, \qquad z_{22} = \frac{1}{h_{22}} \tag{2.3}$$

2.2.1.4 *z to h*

$$h_{11} = \frac{\Delta z}{z_{22}}, \qquad h_{12} = \frac{z_{12}}{z_{22}}, \qquad h_{21} = \frac{-z_{21}}{z_{22}}, \qquad h_{22} = \frac{1}{z_{22}} \tag{2.4}$$

where $\Delta z = z_{11}z_{22} - z_{12}z_{21}$.

2.2.2 Conversion between *y* and *s* Parameters

$$s_{11} = \frac{(1 - y_{11})(1 + y_{22}) + y_{12}y_{21}}{(1 + y_{11})(1 + y_{22}) - y_{12}y_{21}} \tag{2.5}^{\dagger}$$

$$s_{12} = \frac{-2y_{12}}{(1 + y_{11})(1 + y_{22}) - y_{12}y_{21}} \tag{2.6}^{\dagger}$$

$$s_{21} = \frac{-2y_{21}}{(1 + y_{11})(1 + y_{22}) - y_{12}y_{21}} \tag{2.7}^{\dagger}$$

$$s_{22} = \frac{(1 + y_{11})(1 - y_{22}) - y_{21}y_{12}}{(1 + y_{11})(1 + y_{22}) - y_{12}y_{21}} \tag{2.8}^{\dagger}$$

$$y_{11} = \left[\frac{(1 + s_{22})(1 - s_{11}) + s_{12}s_{21}}{(1 + s_{11})(1 + s_{22}) - s_{12}s_{21}}\right]\frac{1}{Z_0} \tag{2.9}$$

$$y_{12} = \left[\frac{-2s_{12}}{(1 + s_{11})(1 + s_{22}) - s_{12}s_{21}}\right]\frac{1}{Z_0} \tag{2.10}$$

$$y_{21} = \left[\frac{-2s_{21}}{(1 + s_{11})(1 + s_{22}) - s_{12}s_{21}}\right]\frac{1}{Z_0} \tag{2.11}$$

$$y_{22} = \left[\frac{(1 + s_{11})(1 - s_{22}) + s_{12}s_{21}}{(1 + s_{22})(1 + s_{11}) - s_{12}s_{21}}\right]\frac{1}{Z_0} \tag{2.12}$$

where Z_0 is the characteristic impedance of the transmission lines used in the scattering parameter system, usually 50 Ω.†

†In converting from *y* to *s* parameters, the *y* parameters must first be multiplied by Z_0, and then substituted in the equations for conversion to *s* parameters.

2.2.3 Conversions among Common Emitter, Common Base, and Common Collector Parameters for *y* and *h* Parameters

2.2.3.1 Common Emitter y Parameters in Terms of Common Base and Common Collector y Parameters

$$y_{11e} = y_{11b} + y_{12b} + y_{21b} + y_{22b} = y_{11c} \tag{2.13}$$

$$y_{12e} = -(y_{12b} + y_{22b}) = -(y_{11c} + y_{12c}) \tag{2.14}$$

$$y_{21e} = -(y_{21b} + y_{22b}) = -(y_{11c} + y_{21c}) \tag{2.15}$$

$$y_{22e} = y_{22b} = y_{11c} + y_{12c} + y_{21c} + y_{22c} \tag{2.16}$$

2.2.3.2 Common Base y Parameters in Terms of Common Emitter and Common Collector y Parameters

$$y_{11b} = y_{11e} + y_{12e} + y_{21e} + y_{22e} = y_{22c} \tag{2.17}$$

$$y_{12b} = -(y_{12e} + y_{22e}) = -(y_{21c} + y_{22c}) \tag{2.18}$$

$$y_{21b} = -(y_{21e} + y_{22e}) = -(y_{12c} + y_{22c}) \tag{2.19}$$

$$y_{22b} = y_{22e} = y_{11c} + y_{12c} + y_{21c} + y_{22c} \tag{2.20}$$

2.2.3.3 Common Collector y Parameters in Terms of Common Emitter and Common Base y Parameters

$$y_{11c} = y_{11e} = y_{11b} + y_{12b} + y_{21b} + y_{22b} \tag{2.21}$$

$$y_{12c} = -(y_{11e} + y_{12e}) = -(y_{11b} + y_{21b}) \tag{2.22}$$

$$y_{21c} = -(y_{11e} + y_{21e}) = -(y_{11b} + y_{12b}) \tag{2.23}$$

$$y_{22c} = y_{11e} + y_{12e} + y_{21e} + y_{22e} = y_{11b} \tag{2.24}$$

2.2.3.4 Common Emitter h Parameters in Terms of Common Base and Common Collector h Parameters

$$h_{11e} = \frac{h_{11b}}{(1 + h_{21b})(1 - h_{12b}) + h_{22b}h_{11b}} \approx \frac{h_{11b}}{1 + h_{21b}} = h_{11c} \tag{2.25}$$

$$h_{12e} = \frac{h_{11b}h_{22b} - h_{12b}(1 + h_{21b})}{(1 + h_{21b})(1 - h_{12b}) + h_{22b}h_{11b}} \approx \frac{h_{11b}h_{22b}}{1 + h_{21b}} - h_{12b}$$

$$= 1 - h_{12c} \tag{2.26}$$

$$h_{21e} = \frac{-h_{21b}(1 - h_{12b}) - h_{22b}h_{11b}}{(1 + h_{21b})(1 - h_{12b}) + h_{22b}h_{11b}} \approx \frac{-h_{21b}}{1 + h_{21b}}$$

$$= -(1 + h_{21c}) \tag{2.27}$$

$$h_{22e} = \frac{h_{22b}}{(1 + h_{21b})(1 - h_{12b}) + h_{22b}h_{11b}} \approx \frac{h_{22b}}{1 + h_{21b}} = h_{22c} \tag{2.28}$$

2.2.3.5 *Common Base h Parameters in Terms of Common Emitter and Common Collector h Parameters*

$$h_{11b} = \frac{h_{11e}}{(1 + h_{21e})(1 - h_{12e}) + h_{11e}h_{22e}} \approx \frac{h_{11e}}{1 + h_{21e}}$$

$$= \frac{h_{11c}}{h_{11c}h_{22c} - h_{21c}h_{12c}} \approx \frac{-h_{11c}}{h_{21c}} \tag{2.29}$$

$$h_{12b} = \frac{h_{11e}h_{22e} - h_{12}(1 + h_{21e})}{(1 + h_{21e})(1 - h_{12e}) + h_{11e}h_{22e}} \approx \frac{h_{11e}h_{22e}}{1 + h_{21e}} - h_{12e}$$

$$= \frac{h_{21c}(1 - h_{12c}) + h_{11c}h_{22c}}{h_{11c}h_{22c} - h_{21c}h_{12c}} \approx (h_{12c} - 1) - \frac{h_{11c}h_{22c}}{h_{21c}} \tag{2.30}$$

$$h_{21b} = \frac{-h_{21e}(1 - h_{12e}) - h_{11e}h_{22e}}{(1 + h_{21e})(1 - h_{12e}) + h_{11e}h_{22e}} \approx \frac{-h_{21e}}{1 + h_{21e}}$$

$$= \frac{h_{12c}(1 + h_{21c}) - h_{11c}h_{22c}}{h_{11c}h_{22c} - h_{21c}h_{12c}} \approx \frac{-(1 + h_{21c})}{h_{21c}} \tag{2.31}$$

$$h_{22b} = \frac{h_{22e}}{(1 + h_{21e})(1 - h_{12e}) + h_{11e}h_{22e}} \approx \frac{h_{22e}}{1 + h_{21e}}$$

$$= \frac{h_{22c}}{h_{11c}h_{22c} - h_{21c}h_{12c}} \approx \frac{h_{22c}}{h_{21c}} \tag{2.32}$$

2.2.3.6 *Common Collector h Parameters in Terms of Common Base and Common Emitter h Parameters*

$$h_{11c} = \frac{h_{11b}}{(1 + h_{21b})(1 - h_{12b}) + h_{22b}h_{11b}} \approx \frac{h_{11b}}{1 + h_{21b}} - h_{11e} \tag{2.33}$$

$$h_{12c} = \frac{1 - h_{21b}}{(1 + h_{21b})(1 - h_{12b}) + h_{22b}h_{11b}} \approx 1 = 1 - h_{12e} \tag{2.34}$$

$$h_{21c} = \frac{h_{12b} - 1}{(1 + h_{21b})(1 - h_{12b}) + h_{22b}h_{11b}} \approx \frac{1}{1 + h_{21b}}$$
$$= -(1 + h_{21e}) \tag{2.35}$$

$$h_{22c} = \frac{h_{22b}}{(1 + h_{21b})(1 - h_{12b}) + h_{22b}h_{11b}} \approx \frac{h_{22b}}{1 + h_{21b}}$$
$$= h_{22e} \tag{2.36}$$

2.2.4 The Application of Two-Port Parameter Types

The z parameters are used principally in network analysis. Very often the feedback network is most conveniently expressed in z parameters.

The h parameters are used for describing transistor characteristics.

The y and s parameters are used for describing network and transistor performance. Except for h_{21e}, the h parameters are gradually becoming obsolete. The s parameters, the scattering coefficients, were originally used at microwave frequencies but are becoming more popular at much lower frequencies. Very often because of their ease of measurement, the s parameters are measured and the y and h parameters are then calculated using the conversion formulas.

2.2.5 Important Relationships for Transistor Parameters of Different Types

Obviously, the parameters of the same type are independent quantities. Some parameters have had long histories and often are used in other transistor models by other names. In addition, some parameters of one type have particularly important relationships to parameters of other types. Some examples of both kinds are

$$\beta \equiv h_{fe} \equiv h_{21e} \tag{2.37}$$

$$\beta_o = h_{FE} \equiv h_{fe} \quad \text{at low frequencies} \tag{2.38}$$

$$\alpha \equiv h_{fb} \equiv h_{21b} \tag{2.39}$$

$$\beta = \frac{\alpha}{1 - \alpha} \approx \frac{1}{1 - \alpha} \quad \text{up to reasonably high frequencies} \tag{2.40}$$

$\alpha \approx 1$, while β has a large range of values especially when $\alpha \to 1$. (2.41)

$$g_{m_0} \equiv y_{21e} \equiv y_{fe} \tag{2.42}$$

$$g_{m_0} = \frac{\beta}{h_{ie}} = \beta y_{ie} \tag{2.43}$$

where g_{m_0} denotes the value of g_m at small-signal conditions or

$$\beta = \frac{g_{m_0}}{y_{ie}} \tag{2.43a}$$

Often the symbol β is used for $|\beta|$ and great care must be exercised in determining what is meant.

Several important characteristics of the above quantities are:

All except h_{FE} are complex quantities and are strong functions of the dc emitter current and the operating frequency. (Some are also weak or strong functions of the dc voltages as indicated in Table 2.1.)

Even though these quantities were derived for a specific transistor configuration, for example, common emitter, they are valid for all circuit configurations using the appropriate transformations.

2.2.6 Typical Two-Port Parameter Data Sheets

Figures 2.2, 2.3, and 2.4 have been included to give the reader some quantitative knowledge of bipolar transistor behavior in terms of y and h parameters. These figures also demonstrate the forms in which the data are presented.

A study of the data of the latter figures, which is substantial, shows that it does not describe the complete range of operation and tremendous amounts of additional data are required to do so.

The parameter concepts are very useful for the analysis of the total circuitry, but the amount of data required to fully present the transistor characteristics is enormous, particularly if the large-signal performance is to be considered. It is obviously desirable to have a transistor model from which one can calculate with reasonable accuracy the important transistor characteristics under varying conditions. Such a model is the well-known hybrid-PI.

2.3 THE SMALL-SIGNAL COMMON EMITTER HYBRID-PI MODEL OF THE BIPOLAR TRANSISTOR

2.3.1 General Discussion

Figure 2.5 shows the small-signal hybrid-PI common emitter model of the intrinsic transistor which is that part of the complete transistor which performs the amplification function.

g'_{m_0} theoretically has the remarkable property quantitatively common to all bipolar transistors in that its value is a function only of the emitter current and the temperature and is given by

$$g'_{m_0} \approx \frac{1}{r_{e_0}} \tag{2.44}$$

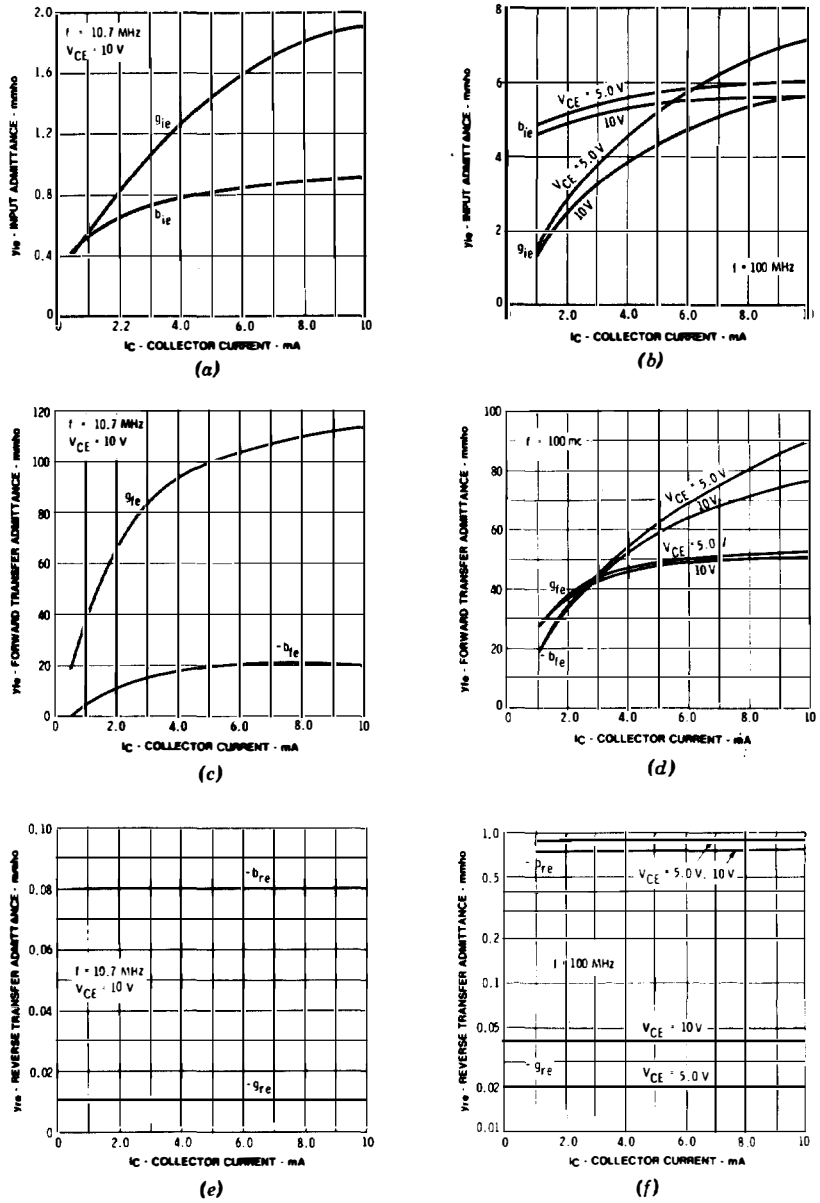

Figure 2.2 2N918. Common emitter y parameters. (a) Input admittance versus I_C at 10.7 MHz. (b) Input admittance versus I_C at 100 MHz. (c) Forward admittance versus I_C at 10.7 MHz. (d) Forward admittance versus I_C at 100 MHz. (e) Reverse admittance versus I_C at 10.7 MHz. (f) Reverse admittance versus I_C at 100 MHz. (g) Output admittance versus I_C at 10.7 MHz. (h) Output admittance versus I_C at 100 MHz. (i) Input admittance versus frequency. (j) Forward admittance versus frequency. (k) Reverse admittance versus frequency. (l) Output admittance versus frequency. (Courtesy of Fairchild Semiconductor.)

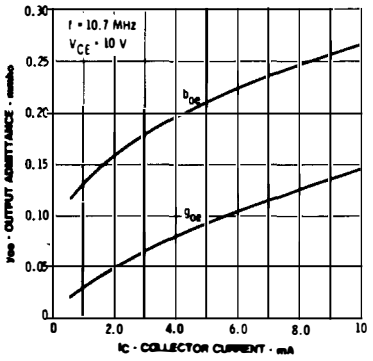

(g)

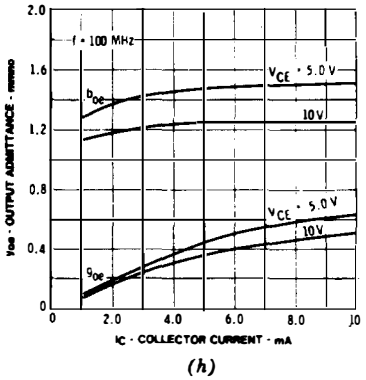

(h)

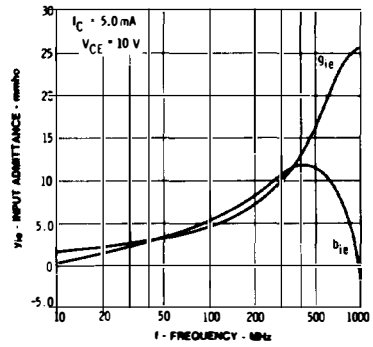

(i)

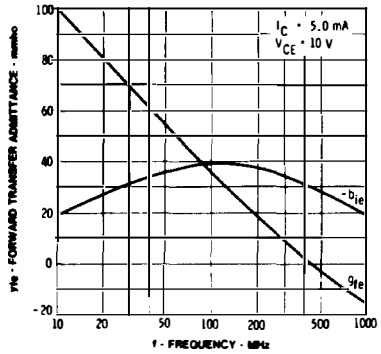

(j)

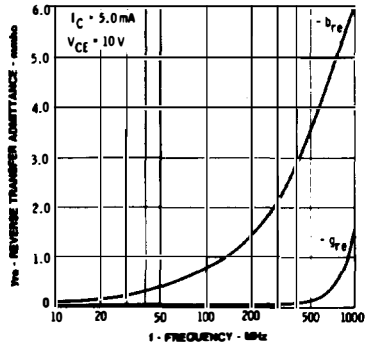

(k)

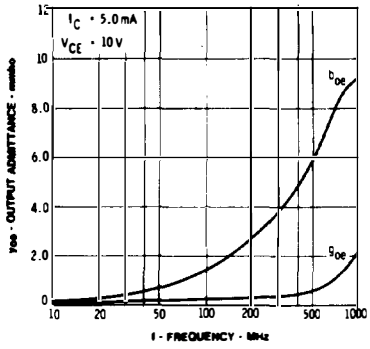

(l)

Figure 2.2 (Continued).

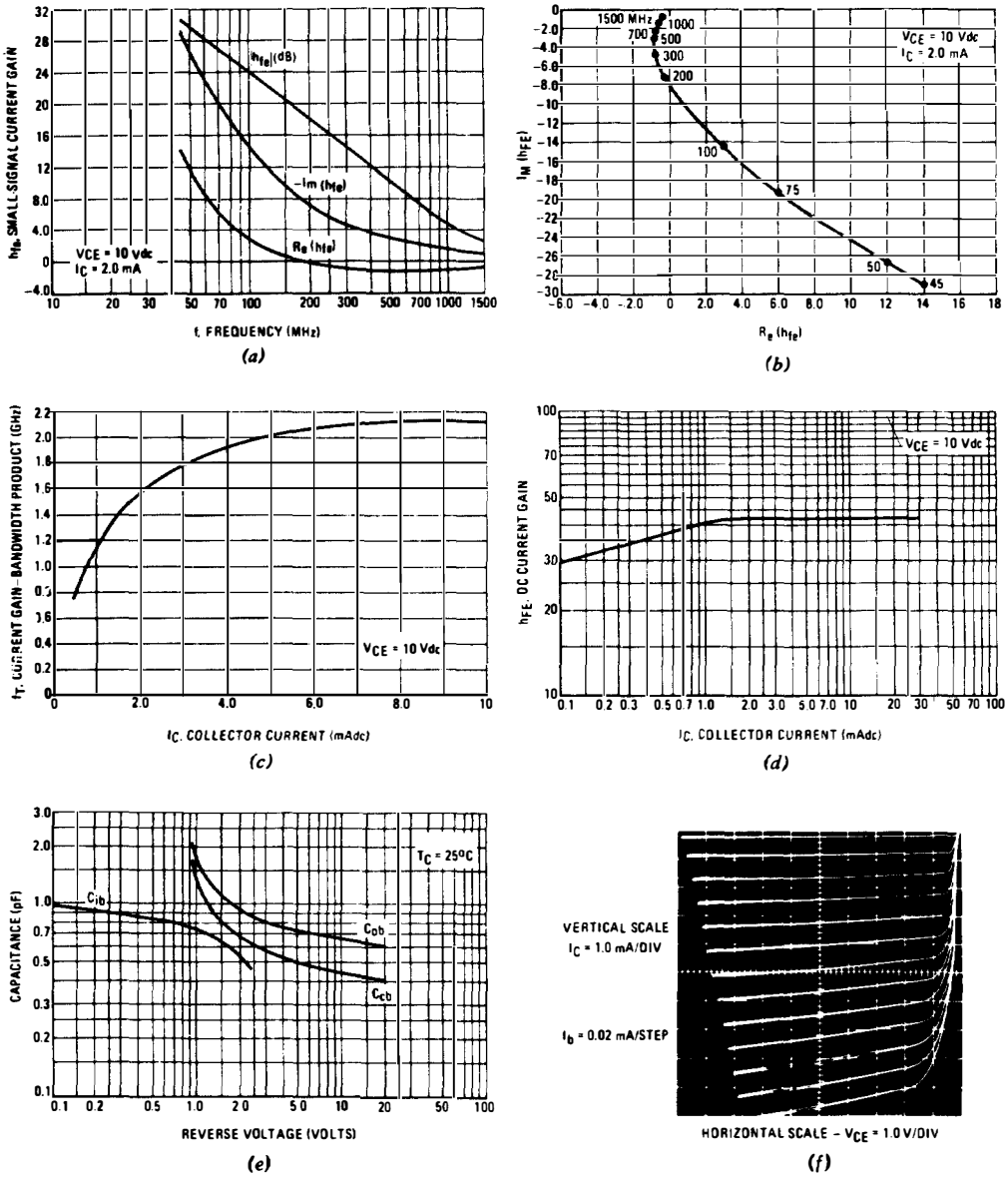

Figure 2.3 2N4957 characteristics. (*a*) h_{fe} versus frequency. (*b*) Polar h_{fe} versus frequency. (*c*) f_T versus I_C. (*d*) h_{FE} versus I_C. (*e*) Capacitance versus reverse voltage. (*f*) Collector characteristics. (*g*) y_{ie} versus frequency. (*h*) Polar y_{ie} versus frequency. (*i*) y_{fe} versus frequency. (*j*) Polar y_{fe} versus frequency. (*k*) y_{oe} versus frequency. (*l*) Polar y_{oe} versus frequency. (*m*) y_{re} versus frequency. (*n*) Polar y_{re} versus frequency. (*o*) y_{ib} versus frequency. (*p*) Polar y_{ib} versus frequency. (*q*) y_{fb} versus frequency. (*r*) Polar y_{fb} versus frequency. (*s*) y_{ob} versus frequency. (*t*) Polar y_{ob} versus frequency. (*u*) y_{rb} versus frequency. (*v*) Polar y_{rb} versus frequency. (*w*) y_{ie} versus I_C. (*x*) y_{ib} versus I_C. (*y*) y_{fe} versus I_C. (*z*) y_{fb} versus I_C. (*aa*) y_{oe} versus I_C. (*bb*) y_{ob} versus I_C. (*cc*) y_{re} versus I_C. (*dd*) y_{rb} versus I_C. (Courtesy of Motorola Inc.)

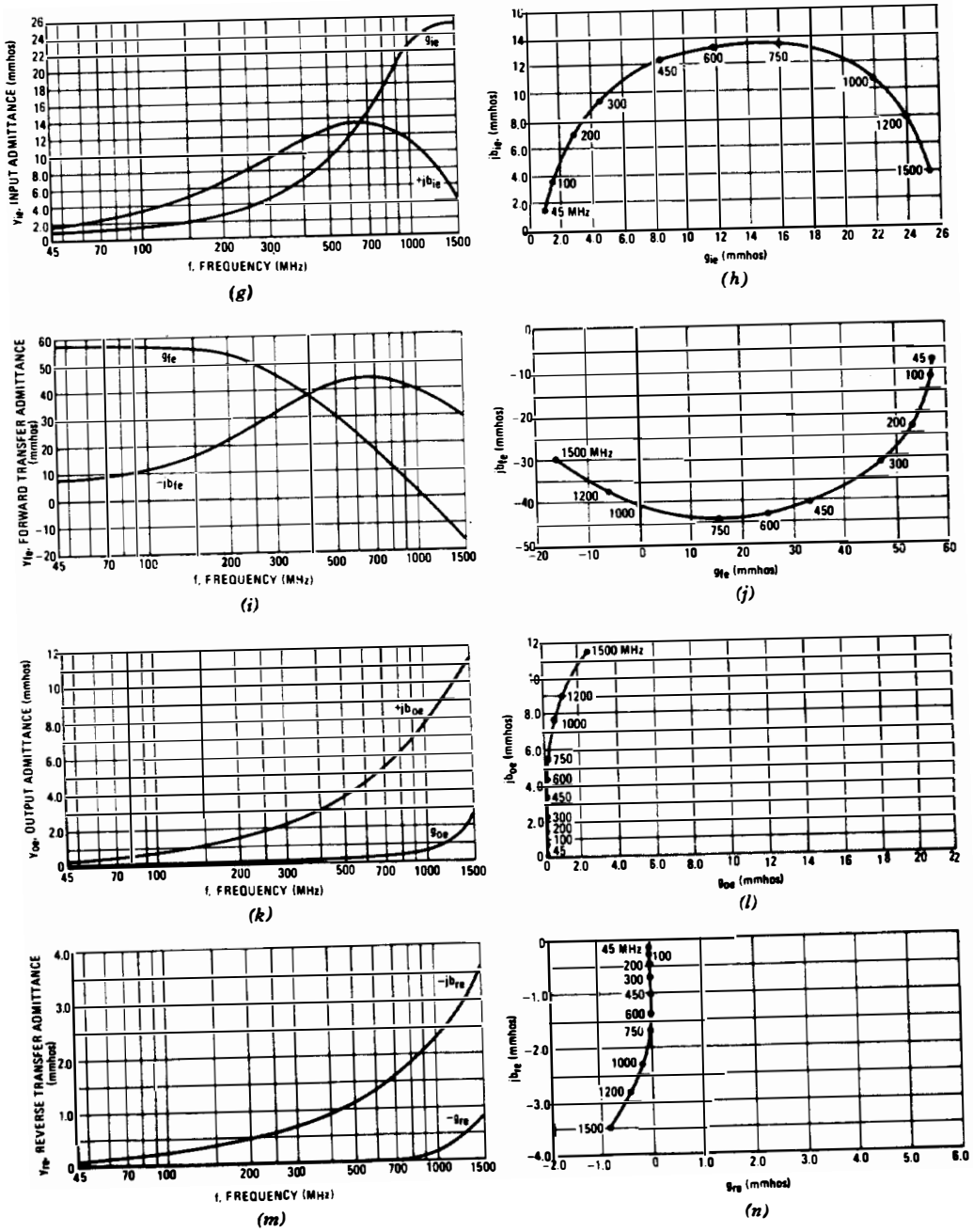

Figure 2.3 (Continued).

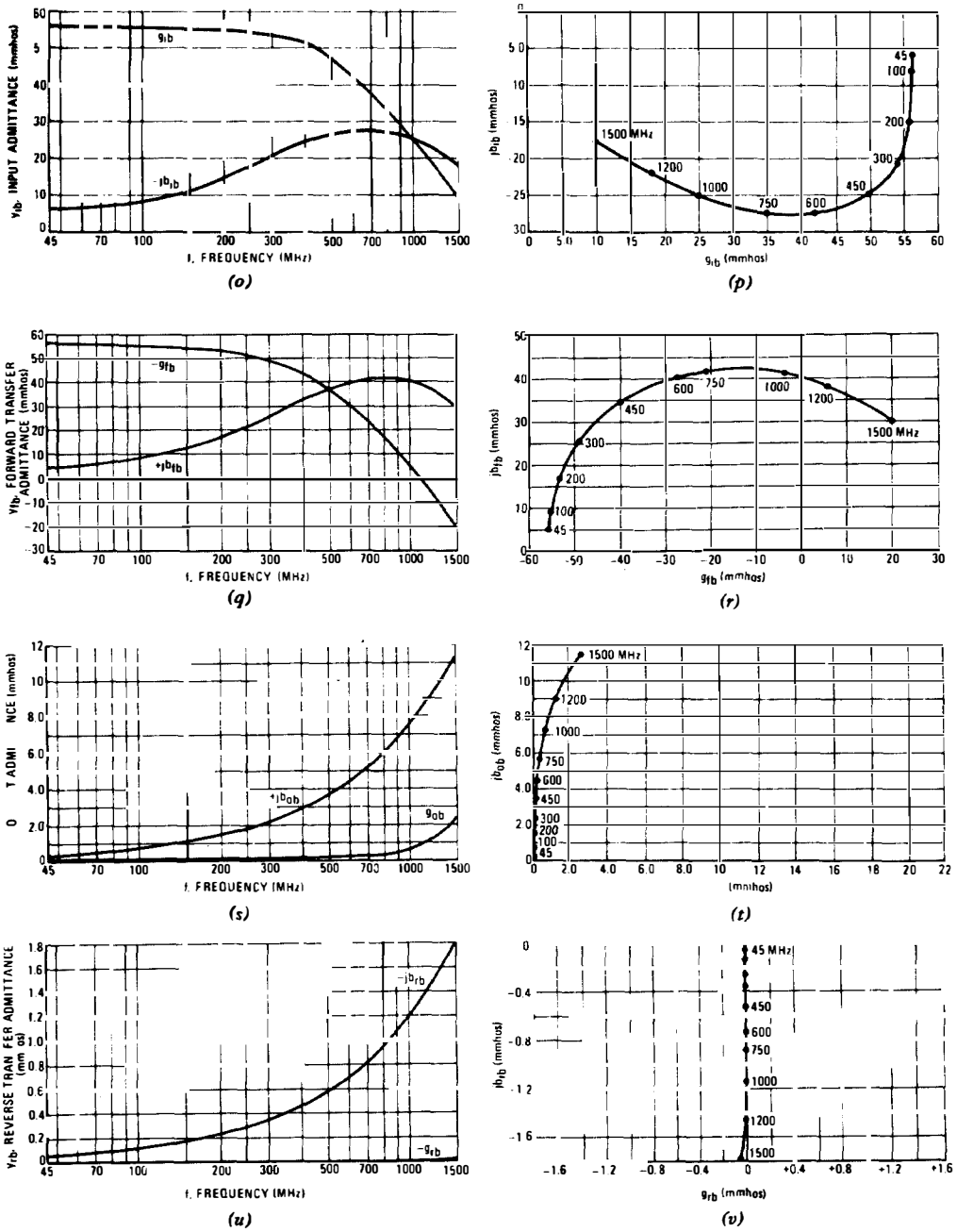

Figure 2.3 (Continued).

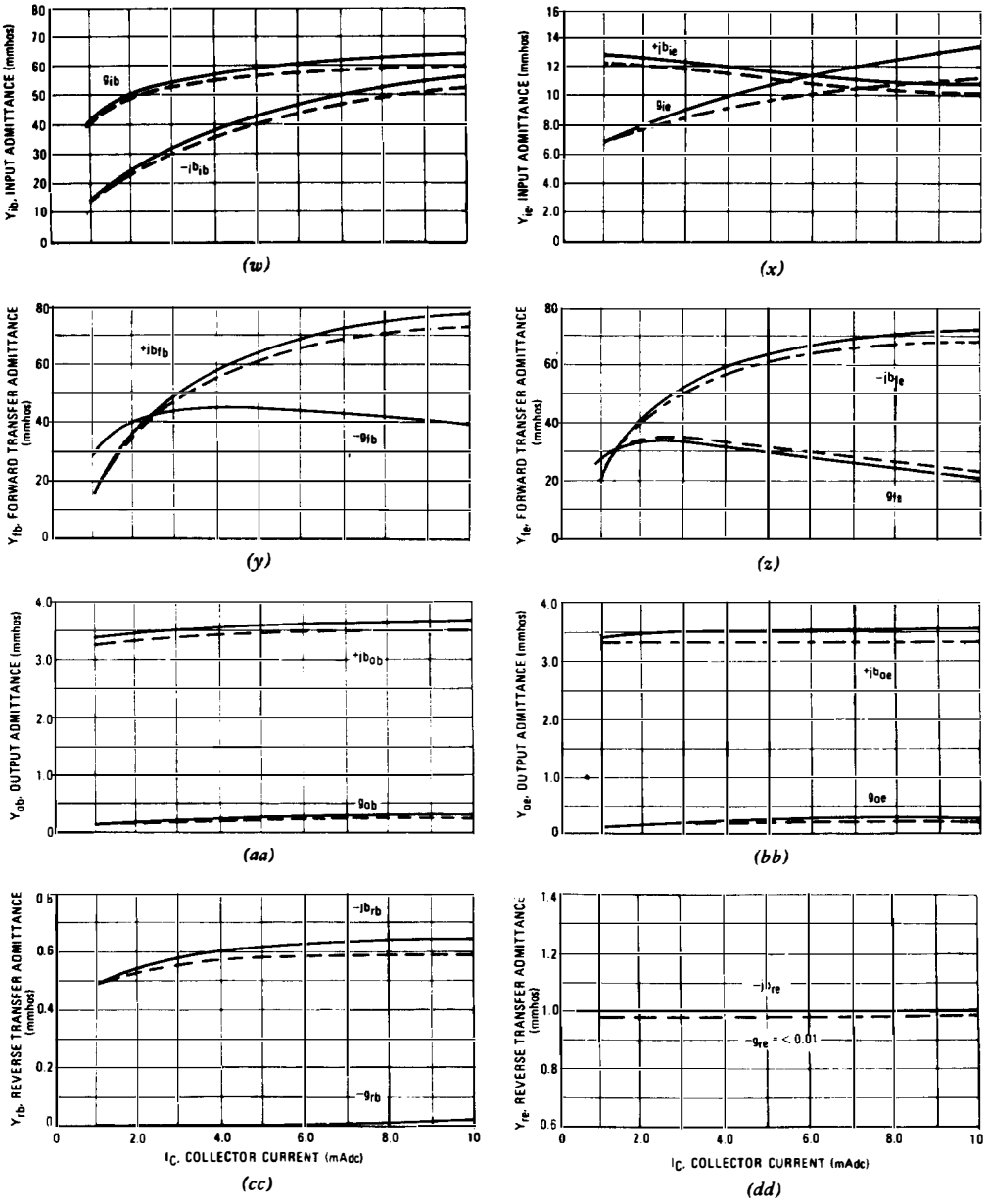

Figure 2.3 (Continued).

2N2857 JAN (*a*) TYPICAL COMMON EMITTER *Y*-PARAMETERS AT 25°C LEAD TEMPERATURE V_{CE} = 6.0 VOLTS, MAGNITUDE IN MILLIMHOS									
FREQUENCY	I_c	INPUT ADMITTANCE		FORWARD TRANSFER ADMITTANCE		REVERSE TRANSFER ADMITTANCE		OUTPUT ADMITTANCE	
(MHz)	(mA)	Y_{ie}	ϕ_{yie}	Y_{fe}	ϕ_{ie}	Y_{re}	ϕ_{yre}	Y_{oe}	ϕ_{yoe}
100	1.0	3.9	78°	34.7	−12°	0.48	−92°	1.2	84°
	1.5	5.1	76°	43.8	−12°	0.48	−90°	1.2	84°
	3.0	7.2	67°	82.1	−20°	0.50	−86°	1.1	78°
	5.0	8.1	63°	110.9	−27°	0.46	−87°	1.2	73°
200	1.0	6.9	74°	35.9	−17°	0.72	−90°	1.8	84°
	1.5	7.7	72°	44.6	−18°	0.72	−92°	1.8	83°
	3.0	10.6	61°	81.0	−29°	0.72	−90°	1.8	80°
	5.0	12.9	53°	108.4	−38°	0.73	−91°	1.7	80°
300	1.0	11.0	69°	35.1	−26°	1.1	−92°	2.7	89°
	1.5	12.0	66°	44.8	−29°	1.1	−94°	2.9	84°
	3.0	15.5	51°	74.3	−43°	1.1	−93°	2.8	83°
	5.0	17.4	43°	91.5	−52°	1.1	−92°	2.8	82°
400	1.0	13.5	66°	35.7	−31°	1.4	−91°	3.4	87°
	1.5	14.6	61°	44.1	−35°	1.4	−93°	3.5	85°
	3.0	17.9	46°	69.1	−50°	1.4	−91°	3.4	83°
	5.0	19.4	38°	82.6	−60°	1.3	−91°	3.4	82°
450	1.0	14.9	60°	35.7	−35°	1.4	−93°	3.8	85°
	1.5	16.2	60°	39.5	−39°	1.4	−90°	3.8	81°
	3.0	19.7	45°	61.0	−55°	1.4	−92°	3.9	78°
	5.0	21.2	37°	78.3	−64°	1.4	−91°	3.7	80°
500	1.0	16.4	59°	35.3	−40°	1.7	−92°	4.1	85°
	1.5	17.6	56°	42.3	−44°	1.7	−91°	4.2	82°
	3.0	20.4	40°	62.4	−61°	1.7	−92°	4.2	82°
	5.0	21.7	33°	71.2	−70°	1.7	−92°	4.1	81°
600	1.0	20.1	53°	35.9	−48°	2.2	−93°	5.0	82°
	1.5	21.0	48°	42.2	−54°	2.1	−93°	5.1	81°
	3.0	22.8	34°	57.3	−70°	2.1	−93°	4.9	82°
	5.0	23.4	27°	63.4	−79°	2.1	−92°	4.8	81°
700	1.0	22.3	50°	37.2	−54°	2.5	−92°	5.7	79°
	1.5	22.8	44°	42.5	−59°	2.5	−92°	5.7	81°
	3.0	24.0	30°	55.1	−75°	2.5	−91°	5.4	81°
	5.0	24.3	24°	59.9	−85°	2.5	−91°	5.4	81°

Figure 2.4 2N2857 JAN. Common emitter characteristics. (Courtesy of Microwave Associates.) (*a*) *y* parameters. These parameters have been calculated from *S*-parameter data measured on a computer controlled network analyzer. (*b*) *h* parameters. These parameters have been calculated from *S*-parameter data measured on a computer controlled network analyzer. The magnitude of h_{ie} is in Ω, and the magnitude of h_{oe} is in $m\Omega^{-1}$.

2N2857 JAN (*b*) TYPICAL COMMON EMITTER *h*-PARAMETERS AT 25°C LEAD TEMPERATURE V_{CE} = 6.0 VOLTS									
FREQUENCY	I_c	SHORT CIRCUIT INPUT IMPEDANCE		FORWARD CURRENT TRANSFER RATIO		REVERSE VOLTAGE TRANSFER RATIO		OPEN CIRCUIT OUTPU T ADMITTANCE	
(MHz)	(mA)	$\lvert h_{ie}\rvert^2$	ϕ_{hie}	h_{fe}	ϕ_{hfe}	h_{re}	ϕ_{hre}	h_{oe}	ϕ_{oe}
100	1.0	254	−78°	8.8	−91°	0.122	10°	4.5	14°
	1.5	195	−76°	8.6	−88°	0.094	13°	4.4	17°
	3.0	137	−67°	11.3	−88°	0.069	25°	6.0	15°
	5.0	122	−63°	13.5	−90°	0.057	29°	6.8	12°
200	1.0	144	−74°	5.2	−92°	0.103	14°	4.2	23°
	1.5	129	−72°	5.8	−91°	0.093	15°	4.6	20°
	3.0	93	−61°	7.6	−91°	0.067	27°	5.9	15°
	5.0	77	−53°	8.3	−91°	0.056	35°	6.5	12°
300	1.0	90	−69°	3.2	−95°	0.107	18°	4.3	30°
	1.5	82	−66°	3.7	−95°	0.092	19°	4.9	28°
	3.0	64	−51°	4.8	−94°	0.075	35°	6.2	19°
	5.0	57	−43°	5.2	−95°	0.067	43°	6.6	16°
400	1.0	73	−66°	2.6	−98°	0.108	22°	4.8	34°
	1.5	68	−61°	3.0	−97°	0.098	25°	5.3	31°
	3.0	55	−46°	3.8	−97°	0.080	41°	6.3	23°
	5.0	51	−38°	4.2	−98°	0.072	49°	6.7	20°
450	1.0	67	−60°	2.4	−96°	0.097	25°	4.9	41°
	1.5	61	−60°	2.4	−99°	0.092	29°	5.2	37°
	3.0	50	−45°	3.0	−100°	0.072	42°	5.8	29°
	5.0	47	−37°	3.6	−101°	0.066	51°	6.2	23°
500	1.0	60	−59°	2.1	−99°	0.106	28°	5.2	40°
	1.5	56	−56°	2.4	−101°	0.098	31°	5.6	35°
	3.0	48	−40°	3.0	−102°	0.084	47°	6.3	27°
	5.0	45	−33°	3.3	−103°	0.079	54°	8.5	23°
600	1.0	49	−53°	1.8	101°	0.110	33°	6.0	42°
	1.5	47	−48°	2.0	−102°	0.103	38°	6.3	38°
	3.0	43	−34°	2.5	−105°	0.096	52°	6.6	28°
	5.0	42	−27°	2.7	−106°	0.093	60°	6.9	25°
700	1.0	44	−50°	1.7	−104°	0.114	38°	6.7	40°
	1.5	43	−44°	1.8	−104°	0.111	43°	6.9	38°
	3.0	41	−30°	2.2	−106°	0.105	57°	7.2	29°
	5.0	41	−24°	2.4	−109°	0.103	64°	7.3	26°

Figure 2.4 (Continued).

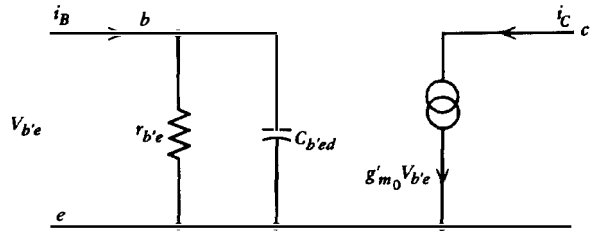

Figure 2.5 Small-signal hybrid-PI intrinsic bipolar common emitter transistor model.

where r_e is the dynamic emitter resistance and, in general, the subscript 0 denotes small signal.

$$r_{e_0} \approx \frac{kT}{qI_E} \tag{2.45}$$

where k is Boltzmann's constant, T is the temperature in degrees Kelvin, q is the charge on the electron, and I_E is the dc emitter current;

$$r_{e_0} = \frac{26\ \Omega}{I_E} \tag{2.45a}$$

at $T = 300°\text{K}$ and I_E in mA.

Other important properties for this model are

$$r_{b'e_0} = \frac{\beta_o}{g'_{m_0}} \tag{2.46}$$

where $\beta_o \equiv h_{fe}$ at low frequer

$C_{b'ed}$ is called the base emi citance and

$$C_{b'ed_0} = \frac{g'_{m_0}(10^6)}{2\pi f_T} \tag{2.47}$$

where f_T is the gain bandwidth product which will be discussed later. C is in pF and f_T is in MHz.

Both β_o and f_T are strong functions of the construction of the transistor and therefore have to be determined for each individual transistor; but it is remarkable that once these two quantities are known, the rest of the model can be calculated.

Experimental investigations of g'_{m_0} have shown that Eqs. (2.44) and (2.45) are not completely true and the model must be modified to agree with experiment.

If the model is analyzed at low frequencies and at small signals, agreement can be obtained by adding a constant r'_e to r_e, called the extrinsic emitter

dynamic resistance, and/or adding a resistance, $r_{bb'}$, called the base spreading resistance in series with the base. Then Eq. (2.45) becomes

$$r_{e_0} = \frac{kT}{qI_E} + r'_e \tag{2.48}$$

For small power transistors, r'_e has been found to vary between 1 and 3 Ω. In this work, for simplicity,

$$r'_e = 1\ \Omega \tag{2.49}$$

so that

$$r_{e_0} = \frac{26T}{I_E T_0} + 1 \tag{2.50}$$

where

$$T_0 = 300°\text{K} \tag{2.50}$$

Figure 2.5 has been modified to become Fig. 2.6*a*. This figure now includes $r_{bb'}$ and capacitors C_{bet}, called the base emitter transition capacitance, $C_{b'c}$, the

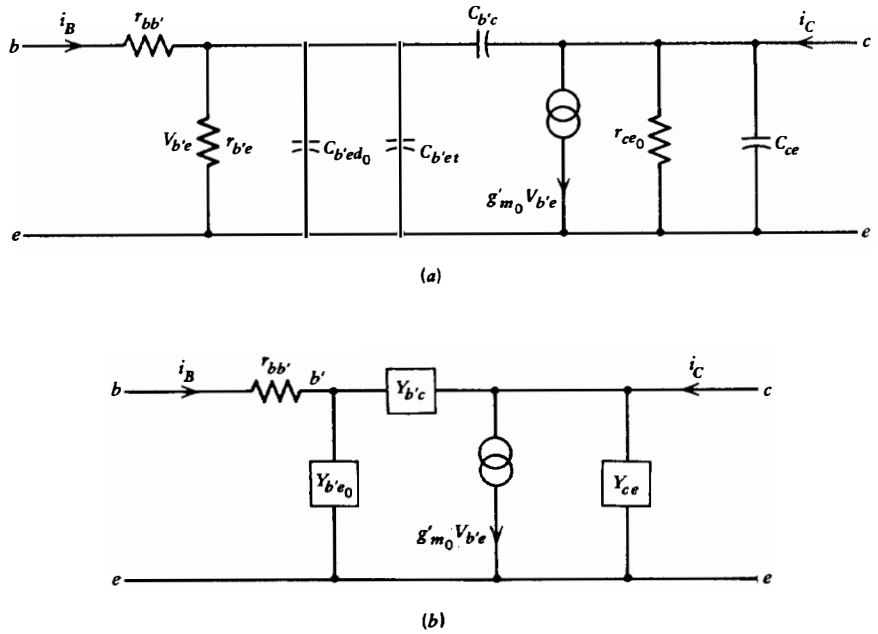

Figure 2.6 Small-signal models of the common emitter bipolar transistor. (*a*) Small-signal model. (*b*) *y* equivalent of (*a*).

capacitance between base and collector, and C_{ce}, the capacitance between collector and emitter. All the latter capacitances are functions of the voltage across them as shown in Fig. 2.3*e*, but they will be considered constant. Also it should be noted that additional capacitances exist because of the transistor packaging but these have been either lumped into the capacitors shown or disregarded as being negligible. Figure 2.6*a* also includes r_{ce} which is necessary to account for the slope of the collector voltage versus collector current characteristic as shown in Fig. 2.3*f*.

Again considering the model of Fig. 2.6*a* at low frequencies and small signals, it is obvious that

$$g_m \equiv \frac{I_e}{V_{be}} = \frac{V_{b'e}}{V_{be}} g'_m \tag{2.51}$$

and from Eq. (2.46)

$$\frac{V_{b'e}}{V_{be}} = \frac{r_{be'}}{r_{b'e} + r_{bb'}} = \frac{\beta_o / g'_{m_0}}{\beta_o / g'_{m_0} + r_{bb'}} \tag{2.52}$$

so that

$$g_{m_0} = \left(\frac{1}{g'_{m_0}} + \frac{r_{bb'}}{\beta_o} \right)^{-1} \tag{2.53}$$

$$= \left(\frac{26T}{I_E T_o} + \frac{r_{bb'}}{\beta_o} + 1 \right)^{-1} \tag{2.54}$$

from Eqs. (2.44) and (2.50).

As noted in Section 2.1, the algorithms specify conditions which make Eq. (2.54) valid for the entire frequency range for which the algorithms will be used.

It should be noted that while $r_{bb'}$ is treated as a constant, it actually varies with frequency and the collector current, being smaller at higher collector currents. Also, while $r_{bb'}$ is considered resistive at some frequencies, it may have a reactive component. It is normally difficult to obtain data for the value of $r_{bb'}$ and it is therefore recommended that for small power transistors, $r_{bb'}$ be assumed to be 60 Ω, which is somewhat pessimistic. A more accurate value of $r_{bb'}$ may be obtained from curves such as in Fig. 2.3*h*, which shows that at the maximum frequency, $y_{i_e} \equiv g_{i_e} \approx 25$ m℧ so that $r_{bb'} = 40$ Ω.

Table 2.1 shows the variation of hybrid-PI parameters with voltage, current, and temperature.

Table 2.1 Variation of Hybrid-PI Parameters with Current, Voltage, and Temperature

	Variation with Increasing...		
Parameter	I_C	V_{CE}	T
g_m	Linear	Independent	Decreases
r_{be}	$1/I_C$	Increases	Increases
C_{be}	Linear	Decreases	Varies with transistor
$r_{bb'}$	Decreases with high current	?	Increases
C_{cb}	Independent	Decreases	Independent
β_o	Independent	Increases slowly	Increases

2.3.2 The Calculation of β from the Model of Fig. 2.6*a*

$$\beta \equiv \left.\frac{I_c}{I_b}\right|_{V_{ce}=0}$$

If C_{be_t} and $C_{b'c}$ are neglected, which is permissible when I_E is reasonably large, then

$$V_{b'e} = I_b\left(\frac{1}{r_{b'e}} + \frac{j}{X_{C_{be_{d_0}}}}\right)^{-1}$$

$$= I_b\left(\frac{g'_{m_0}}{\beta} + \frac{jg'_{m_0}f}{f_T}\right)^{-1} \tag{2.55}$$

from Eqs. (2.46) and (2.47). But $I_c = g'_{m_0}V_{b'e}$, so that from Eq. (2.55)

$$\beta = \left(\frac{1}{\beta_o} + \frac{jg'_{m_0}f}{f_T}\right)^{-1}$$

$$= \frac{\beta_o[1 - j\beta_o f/f_T]}{1 + (\beta_o f/f_T)^2} \tag{2.56}$$

In polar coordinates

$$\beta = \frac{\beta_o}{\sqrt{1 + (\beta_o f/f_T)^2}} \angle \tan^{-1}\left(-\beta_o \frac{f}{f_T}\right) \tag{2.56a}$$

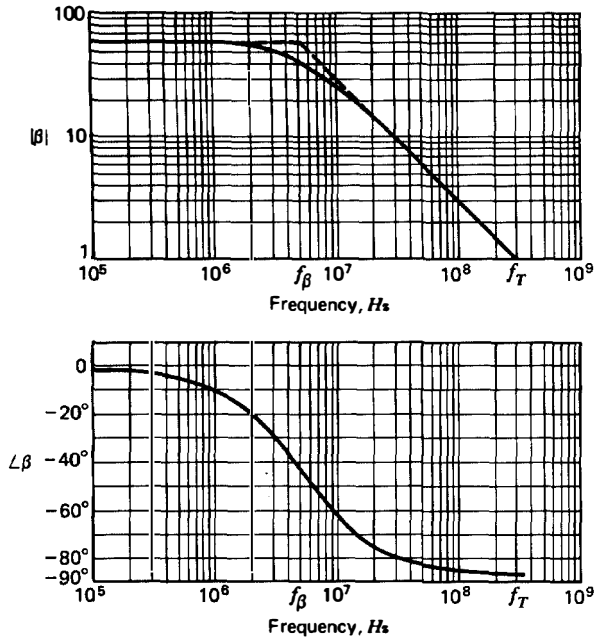

Figure 2.7 Typical magnitude and phase of β versus frequency.

It is seen from Eq. (2.56a) that

$$|\beta| = \beta_o \qquad \text{at } f \approx 0 \tag{2.57a}$$

$$|\beta| = 0.707\beta_o \quad \text{at } f = \frac{f_T}{\beta_o} \equiv f_\beta \tag{2.57b}$$

$$|\beta| = 1 \qquad \text{at } f = f_T \tag{2.57c}$$

Figure 2.7 shows a plot of Eq. (2.56a) for a transistor having a β_o of 60 and an f_T of 300 MHz. This plot is idealized since if measurements were taken, the plot would be valid up to some frequency between f_β and f_T and would be completely inaccurate near f_T because of stray elements in the transistor. Thus f_T should be considered as an extrapolated value from data taken at some frequency above f_β where the ideal curve of $|\beta|$ versus f is a straight line of slope -1.

For example, the plot gives $\beta = 10$ at $f = 30$ MHz. Therefore, f_T would extrapolate to $30 \times 10 = 300$ MHz. The same procedure would be followed in determining f_T from a transistor data sheet where $|\beta| \equiv |h_{fe}|$ is specified at some arbitrary high frequency.

It should be noted that f_T is a function of both the currents and voltages in the transistor, so that efforts should be made to obtain f_T at the correct

operating conditions. However, if the assumed operating conditions are somewhat inaccurate, the resulting errors will not be terribly significant.

Figures 2.3*a* and 2.3*b* show plots of $|\beta|$ versus frequency and Fig. 2.3*c* shows the plot of f_T versus collector current. These figures are presented to give some idea of how these parameters vary in a high-frequency transistor suitable for oscillators.

Figure 2.4*b* shows the variation of h_{fe} for different values of current and frequency in polar form. Equation (2.56a) states that the maximum absolute value of the phase angle is 90°, while Fig. 2.4*b* shows larger angles at the very high frequencies, which means that the model is insufficiently accurate at these frequencies. But, this transistor is not used at a frequency higher than 100 MHz where $f_T \approx 1100$ MHz. If it is assumed that $\beta_o = 100$, then $\tan^{-1}\theta = 10$ and θ is 85°, which is not far from the indicated value of $\approx 88°$.

2.3.3 The Calculation of y_{ie} from the Model of Fig. 2.6*a*

Neglecting C_{bet} and $C_{b'c}$, it is seen by inspection that

$$y_{ie} = \frac{(1/r_{bb'})\left[1/r_{b'e} + j/X_{C_{b'ed_0}}\right]}{1/r_{bb'} + 1/r'_{be} + 1/X_{C_{b'ed_0}}}$$

$$= \frac{(1/r_{bb'})\left[g'_{m_0}/\beta_o + jg'_{m_0}f/F_T\right]}{(1/r_{bb'} + g'_{m_0}/\beta_o) + jg'_{m_0}f/f_T} \tag{2.58}$$

Equation (2.58) is rather complicated and it is better to put it into polar form:

$$y_{ie} = \frac{(g'_{m_0}/r_{bb'}\beta_o)\sqrt{1 + (\beta_o f/f_T)^2}}{\sqrt{(1/r_{bb} + g'_{m_0}/\beta_o)^2 + (g'_{m_0}f/f_T)^2}} \tag{2.58a}$$

at an angle

$$\tan^{-1}\frac{\beta_o f}{f_T} - \tan^{-1}\frac{\beta_o f/f_T}{(1 + \beta/r_{bb'}g'_{m_0})}$$

Equation (2.58a) is also complicated, but is is evident from the angle term that the angle is always positive but its absolute magnitude first increases with frequency and then decreases until it approaches 0, as shown in Figs. 2.3*g*, 2.3*h*, and 2.4*a*.

2.3.4 The Calculation of y_{21e}, y_{12e}, and y_{22e} from the Model of Fig. 2.6*a*

The calculation of $y_{21e} \equiv y_{fe}$ can most easily be performed with the aid of Eq. (2.43) which states

$$y_{fe} \equiv g_{m_0} = \beta y_{ie} \tag{2.59}$$

This can be done by multiplying the results of Eqs. (2.56a) and (2.58a). The form of the absolute magnitude is rather complicated and therefore difficult to analyze, but the angle is

$$\tan^{-1}\left(-\frac{\beta_o f}{f_T}\right) + \tan^{-1}\left(\frac{\beta_o f}{f_T}\right) - \tan^{-1}\left(\frac{\beta_o f/f_T}{1 + \beta_o/r_{bb'}g'_{m_0}}\right) = -\tan^{-1}\frac{f/f_T}{1/\beta_o + 1/r_{bb'}g'_{m_0}} \tag{2.59a}$$

which shows that the angle is lagging and its magnitude increases with frequency and with β_o, g'_{m_0}, and $r_{bb'}$, and hence with the dc emitter current.

Figure 2.4*a* shows that the angle at 100 MHz is 12° for a current of 1.5 mA, which is fairly large for a precision oscillator. The 12° angle is not particularly harmful and since the great majority of oscillators in the common emitter transistor configuration will not exceed 50 MHz, it is seen that for all practical purposes, the angle can be considered to be 0° for this particular transistor type.

From inspection,

$$y_{re} \equiv y_{12e} = j2\pi f C_{bc} \tag{2.60}$$

$$y_{oe} \equiv y_{22e} = j2\pi f(C_{bc} + C_{ce}) + \frac{1}{r_{ce}} \tag{2.61}$$

2.3.5 The Effect of Local Feedback upon the Transistor Performance in the Common Emitter Configuration

Local emitter degenerative feedback is often used to stabilize the performance of transistors in the common emitter configuration. The effects of such feedback is studied in this section.

Figure 2.8 shows the schematic of a transistor, the emitter of which is fed to a resistor R_E and the end of the resistor serves as the common connection point.

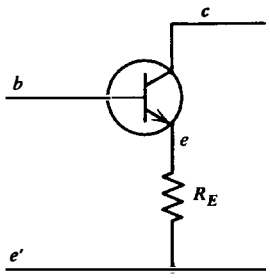

Figure 2.8 Transistor local emitter degeneration.

Figure 2.9 shows the two-port equivalent of Fig. 2.8 and the problem is to calculate the equivalent network Y_c which is composed of networks $Y_A + Y_B$ in series. This can be done in a straightforward manner as follows:

1 Transform the Y networks into Z networks.
2 Add the corresponding parameters to obtain Z_c.
3 Transform the Z_c network into the equivalent Y_c network.

The above procedure is very straightforward but is tedious and laborious and gives little insight into what is happening to the various elements in the hybrid-PI model.

A better procedure is to deal directly with the hybrid-PI model. In this case, Fig. 2.6*b* becomes Fig. 2.10.

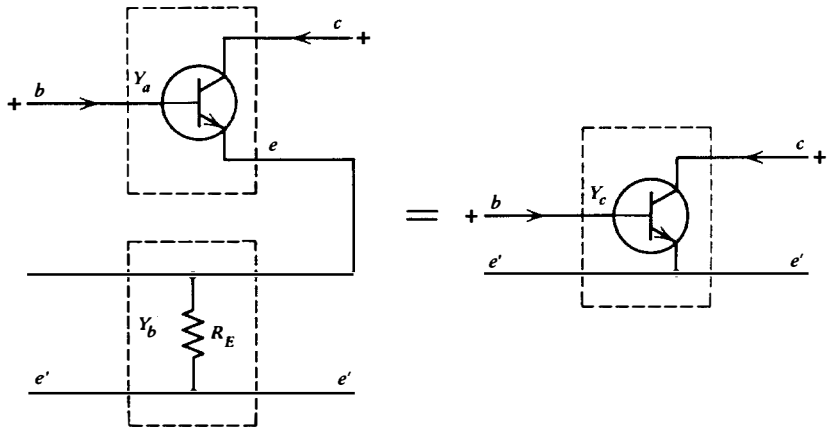

Figure 2.9 Two-port equivalent of Fig. 2.8.

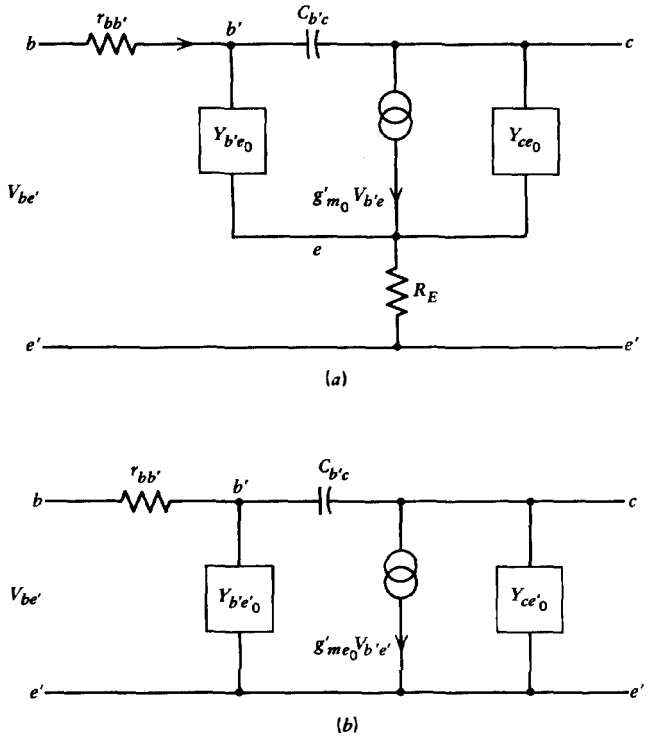

Figure 2.10 Hybrid-PI model of emitter degeneration. (*a*) PI model. (*b*) Equivalent of (*a*).

Analysis of the circuit in Fig. 2.10*a* using mesh analysis results in the following at *frequencies well below* f_T (See Fig. 2.10b):

1 β, $r_{bb'}$, and $C_{b'c}$ are unchanged. (2.62)

2 $$Y_{be'} = Y_{b'e}\left(1 + \frac{R_E}{r_e}\right)^{-1}. \tag{2.63}$$

3 Similarly, $$Y_{ce'} = Y_{ce}\left(1 + \frac{R_E}{r_e}\right)^{-1}. \tag{2.64}$$

4 $$g'_{me_0} = g'_{m_0}\left(1 + \frac{R_E}{r_e}\right)^{-1}. \tag{2.65}$$

5 Equation (2.58a) shows that $y_{ie'}$ is decreased to a degree strongly dependent upon $r_{bb'}$.

6 Equation (2.59) shows that $y_{fe'}$ is decreased both in magnitude and phase.

It is noteworthy that the above results can be obtained by merely substituting $r_e + R_e$ for r_e where r_e is defined in Eq. (2.50).

2.4 LARGE-SIGNAL COMMON EMITTER BIPOLAR TRANSISTOR CHARACTERISTICS

2.4.1 Introduction

The parameters described up to now are valid only for small V_{be} signals up to about 10 mV. Some special cases of large signal characteristics will now be briefly treated. The treatment is based upon the work described by Holford in Ref. 2.1 and is further explained by Clarke and Hess in Ref. 2.3 and Frerking in Ref. 1.10. The treatment will only broadly present the derivation and the final results. Those interested in more detail may consult the cited references.

2.4.2 Basis and Results of the Derivation

The derivation is based upon the intrinsic model first shown in Fig. 2.5 and now repeated in Fig. 2.11 with slight changes in nomenclature. It is important to note that the derivation is valid only when $r_{bb'}$ and r_e' can be neglected.

It will be noted that some of the elements in Fig. 2.6 are absent in Fig. 2.11. This has been done to make the mathematics less complicated. Therefore, use of the results should include provisions for the missing elements or the circuits should operate at conditions where the missing elements are unimportant.

The derivation is as follows:

1 The results are assumed independent of V_{CE}. This assumption requires that $V_{CE} > 1.4(V_L + V_b)$.

2 β is assumed to be large, therefore

$$i_E \approx i_C$$

3 $r_{bb'}$ and $r_e' = 0$, by assumption.

4 $i_E = I_E + \sum_{M=1}^{M} I_{e_M} \cos(M\omega t)$ (2.66)
Using standard notation, I_E is the mean emitter current, I_{e_M} is the rms component at frequency Mf; for example, I_{e_1} is the fundamental current.

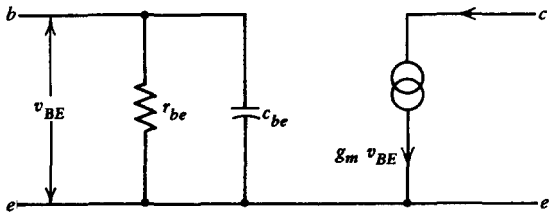

Figure 2.11 Hybrid-PI common emitter bipolar transistor model for determination of large-signal characteristics.

5 $v_{BE} = V_{BE} + \sqrt{2}\, V_{be}(\cos \omega t)$ (2.67)
It is very important that the ac component V_{be} be highly sinusoidal, otherwise the results are not valid.

6 $i_E = K_1 e^{K_2 v_{BE}}$ (2.68)
where K_1 and K_2 are constants of the transistor but functions of the temperature.

7 I_E and I_{e_M} for $M = 1$, 2, and 3 are calculated from steps 4 to 6 by Fourier analysis, as functions of V_{be}.

8 From step 7 is calculated the applicable

$$\gamma_M = \frac{I_{e_M}}{I_E} \quad \text{for } M = 1, 2, 3 \tag{2.69}$$

9 The ratio

$$\alpha = \frac{g_m}{g_{m_0}} \tag{2.70}$$

is calculated from the relationship

$$g_m = \frac{I_{e_1}}{V_{be}} \tag{2.71}$$

and

$$g_{m_0} = \frac{I_E}{26} \tag{2.72}$$

from Eqs. (2.44) and (2.45a).

10 The derivation and Eqs. (2.46) and (2.47) also prove that at $T = 300°K$ and neglecting the 1 Ω

$$r_{be} = \frac{r_{be_o}}{\alpha} = \frac{\beta_o}{g_m} \tag{2.73}$$

$$r_{ce} = \frac{r_{ce_0}}{\alpha} \tag{2.74}$$

$$C_{bed} = \alpha C_{bed_0} = \frac{g_m(10^6)}{2\pi f_T} \tag{2.75}$$

where the subscript 0 denotes the small-signal value as shown in Fig. 2.6. Or, in general,

$$Y_{be} = \alpha Y_{be_0} \tag{2.76}$$

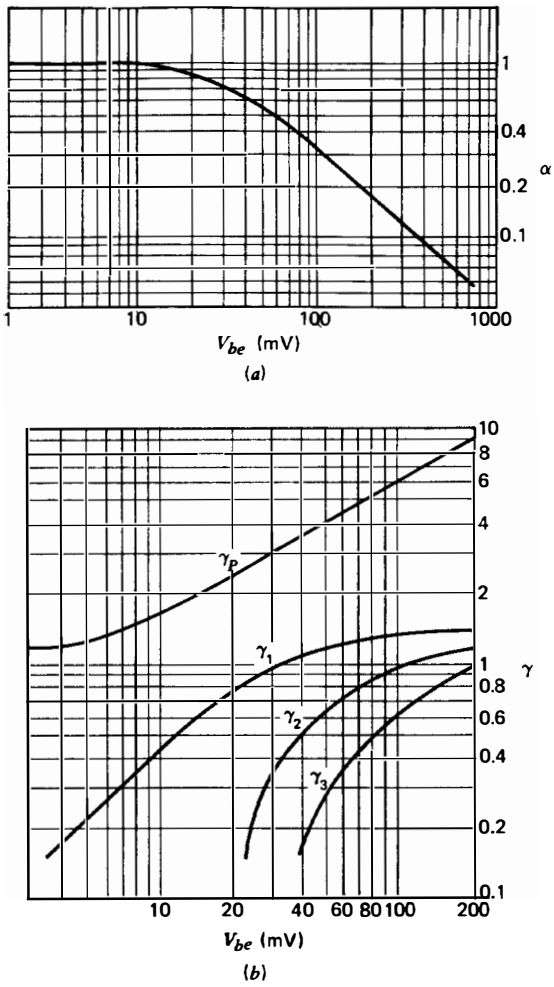

Figure 2.12 Common emitter bipolar transistor large-signal characteristics. (*a*) Variation of α with V_{be}. (*b*) Variation of γ with V_{be}.

Equations (2.69) and (2.70) are plotted in Fig. 2.12,† which also includes the plot

$$\gamma_P = \frac{i_{\text{peak}}}{I_E} \tag{2.69a}$$

†Holford, K., "Transistor *LC* Oscillator Circuits," *Mullard Tech. Commun.* 5, p. 19 (Dec. 1959), Figs. 2 and 5 (modified). Reprinted with permission.

From Eqs. (2.70), (2.71), and (2.72) one obtains the interesting relationship

$$\gamma_1 = \frac{\alpha V_{be}}{26} \tag{2.77}$$

From the curves, it is seen that for $\alpha \leqq 0.3$,

$$\gamma_1 \approx 1.4 \tag{2.78}$$

therefore,

$$\alpha V_{be} \approx 36 \text{ mV} \tag{2.79}$$

Equation (2.79) is valid for $\alpha < 0.7$, where $\gamma \approx 1.4$ as shown in Figs. 2.12*a* and 2.12*b*.

It should be noted that all of the above relationships apply at $T = 300°K$ and slight revisions must be made for the other temperatures found in practice (-65 to 85°C).

The analysis also shows an accompanying bias shift which tends to increase I_E as V_{be} is increased, but the circuits in this book are so designed that the effect of the bias shift is negligible, so it will not be considered.

Holford in Ref. 2.2 has also proposed similar techniques for transistors with emitter degeneration. Again Holford's work is further explained by Clarke and Hess in Ref. 2.3 and by Frerking in Ref. 1.10. However, this technique is not considered particularly useful except for low-frequency relatively high-power oscillators. It is also much more difficult to apply. For these reasons, it is not discussed further, but the results are summarized in Fig. 2.13.†

The exponential nature of Eq. (2.68) causes the emitter current, i_E, to be composed of pulses the width of which decreases sharply as the magnitude of V_{be} in Eq. (2.67) increases. The effect is due to the cut off of the emitter current during part of the cycle because of the swinging of the base emitter junction below the contact potential. This results in highly efficient conversion of dc power into ac power. This effect is identical to that which occurs in class C amplifiers and multipliers.

Figure 2.12*b* shows that γ_1 is 1.4 for V_{be} greater than 113 mV. Most engineers, when confronted with this relationship, find it very surprising and hard to believe that the fundamental component is greater than the dc current, but many times it has been experimentally demonstrated to be so.

Figure 2.12*b* can also be used in the design of frequency multipliers, and there will be occasion to use this information in Chapter 10.

†Holford, K., "Transistor *LC* Oscillator Circuits," *Mullard Tech. Commun.* 5, p. 64 (Feb. 1960), Fig. 6 (modified). Reprinted with permission.

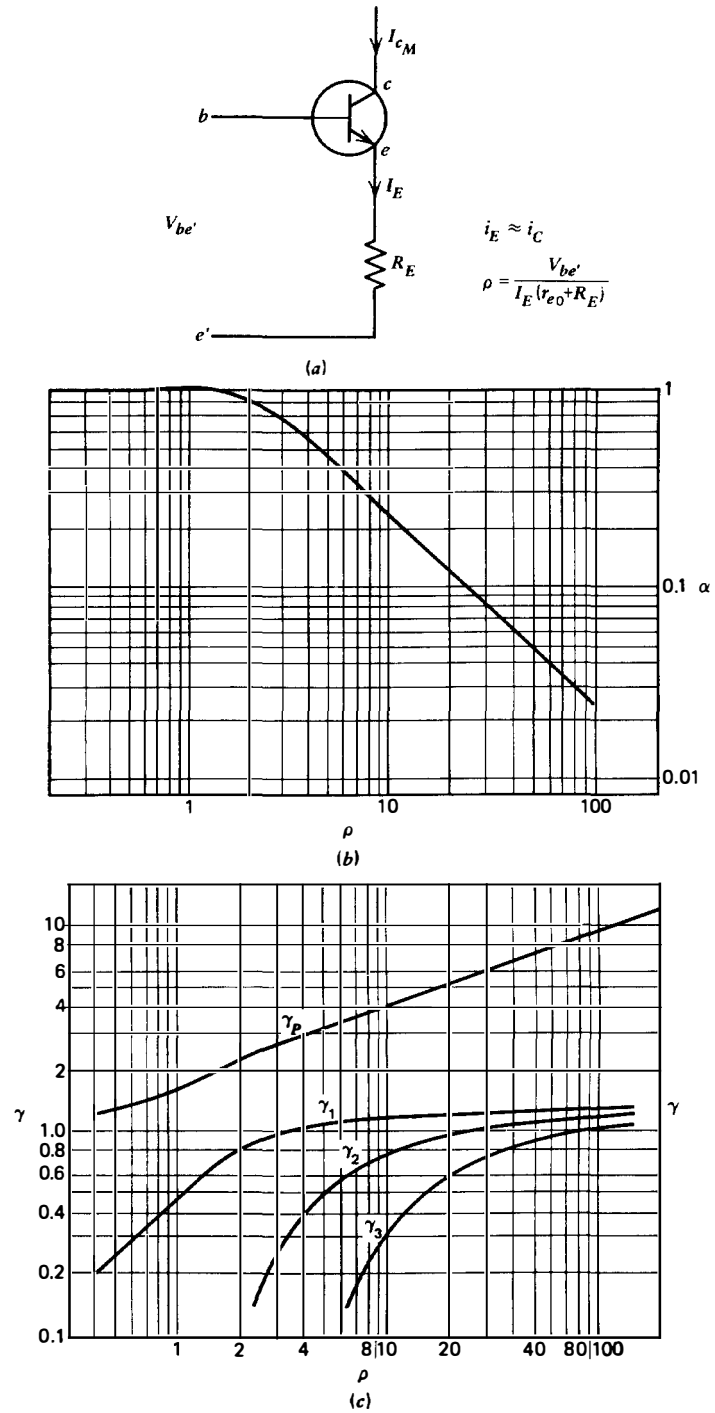

Figure 2.13 Common emitter bipolar transistor large-signal characteristics with emitter degeneration (*a*) Model of circuit and definition of ρ. (*b*) Variation of α with ρ. (*c*) Variation of γ with ρ.

2.5 THE COMMON BASE BIPOLAR TRANSISTOR

There are certain oscillators which find it more convenient to use the transistor in the common base configuration, particularly at high frequencies. The more important characteristics are briefly presented in this section.

2.5.1 Small-Signal Characteristics

2.5.1.1 y Parameters

$$\alpha = h_{21b} \tag{2.80}$$

and from Eq. (2.2)

$$\alpha = \frac{y_{21b}}{y_{11b}} \tag{2.81}$$

Figures 2.3*p* and 2.3*r* show that economical transistors may have

$$\alpha = -1 \tag{2.82}$$

for all frequencies to 200 MHz for $I_C \leqq 2$ mA.

Figure 2.3*p* shows that at $f = 45$ MHz, y_{11b} has a phase angle of about $-5°$ and increases to about $-15°$ at 200 MHz. The minus sign signifies that y_{11b} is inductive.

Equation (2.17) states that

$$y_{11b} = y_{11e} + y_{12e} + y_{21e} + y_{22e} \tag{2.83}$$

$$\simeq y_{21e} \tag{2.83a}$$

for the lower frequencies, where $y_{21e} \gg$ the sum of the remaining terms, which is seen from Figs. 2.3*g*, 2.3*j*, and 2.3*k* to be true up to about 100 MHz; so that for all frequencies < 100 MHz

$$y_{11b} = g_{m_0} \approx \left(\frac{26}{I_E} + 1 + \frac{r_{bb'}}{\beta_0} \right)^{-1} \tag{2.84}$$

from Eq. (2.54) at $T = 300°$K.

Equation (1.33) states that the input Y_{INb},

$$Y_{INb} = y_{11b} - \frac{y_{12b} y_{21b}}{y_{22b} + Y_L} \tag{2.85}$$

and Y_{INb} can be very small depending upon the value of the Y_b parameters and Y_L. This means that under certain conditions the input impedance can be quite

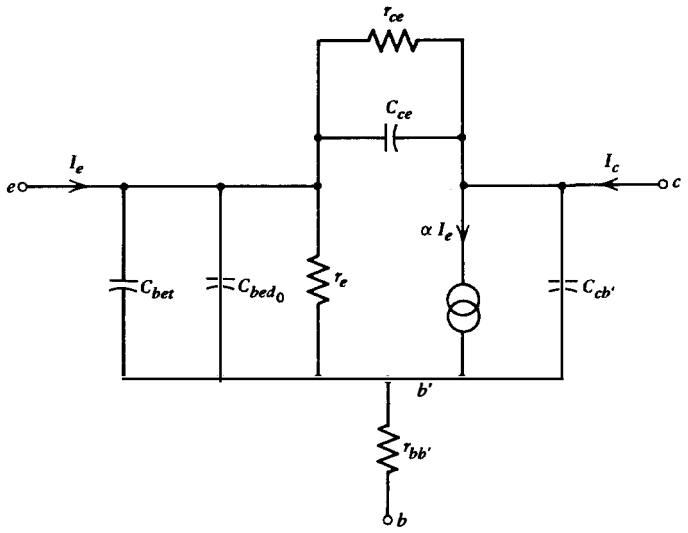

Figure 2.14 Hybrid-PI model of common base bipolar transistor.

large as contrasted to the low input impedance seen at most frequencies and loads. However, this effect will not be strong below 200 MHz in high-performance transistors such as that described in the curves of Fig. 2.3.

2.5.1.2 Hybrid-PI Model for the Common Base Transistor

Figure 2.14 shows a hybrid-PI model of the common base transistor. All symbols in this model, which are identical to those in Fig. 2.6*a*, have the same significance.

The major differences in the two models are shown in Table 2.2.

2.5.2 Large-Signal Characteristics

In general, Eq. (2.83) is still valid, that is,

$$\alpha = -1$$

The other characteristics depend upon whether v_{EB} is sinusoidal or i_E is sinusoidal. Both v_{EB} and i_E can be sinusoidal only in the small-signal case. In the large-signal case v_{EB} is sinusoidal when the emitter base circuit is effectively in parallel with the resonator. Similarly, i_E is sinusoidal in the dual case, that is, the emitter is effectively in series with the resonator.

2.5.2.1 Large-Signal Characteristics for Sinusoidal v_{BE}

The theory developed in Section 2.3 for the common emitter connection is also applicable to the common base connection. The only difference is that g_{m_0}

Table 2.2 Comparison of Common Emitter and Common Base Parameters

Parameter	Common Emitter	Common Base
Useful current generator representation	Characterized by g_m and V_{be}	Characterized by α and I_e
C_{bed_0}	Very important	Not so important as it is shunted by r_e which has a low value. This fact explains the superior high-frequency performance of the common base configuration.
$r_{bb'}$	Limits the high-frequency performance in conjunction with C_{bed_0}	More important in determining the value of y_{11b}
Important feedback capacitance	C_{cb}	C_{ce}

becomes the small-signal input conductance which has the same numerical value as the small-signal transconductance of the common emitter connection.

2.5.2.2 *Large-Signal Characteristics for Sinusoidal i_E*

These are very important for self-limiting oscillators, wherein the resonator circuit, usually a crystal network, is in series with the emitter, such as in the Butler oscillator described in Chapter 11.

In this case, I_e is known and it is desired to compute V_{eb} and the resultant R_{IN}. The method of performing these calculations will now be derived, in accordance with a modified form of the procedure beginning on p. 246 of Ref. 2.3,† as follows:

1 The results are assumed independent of V_{CE}. This assumption requires that $V_{CE} > 1.4(V_L + V_e)$

2 α is assumed ≈ -1 so that

$$i_E \approx -i_C \tag{2.86}$$

3 r_e' and $r_{bb'}$ are assumed negligible so that

$$g_{m_0} = \frac{I_E}{26} \tag{2.87}$$

4 $v_E = V_E + \Sigma_{m\approx 1}^{M} V_{e_M} \cos(M\omega t)$ (2.88)

†Clarke/Hess, *Communication Circuits: Analysis and Design*, © 1971, Addison-Wesley, Reading, Mass. Fig. 6.7-4 (modified). Reprinted with permission.

5 Let

$$i_E = I_E\left(1 + \sqrt{2}\,\frac{I_e}{I_E}\cos\omega t\right) \tag{2.89}$$

$$= I_{ES}e^{K_2 v_{EB}} \tag{2.89a}$$

from which

$$I_{ES}e^{K_2 v_{EB}} = I_E\left(1 + \frac{\sqrt{2}}{I_E}I_e\cos\omega t\right) \tag{2.89b}$$

where I_{ES} is the hypothetical value of I_E at $V_{EB} = 0$ and

$$K_2 = \frac{q}{kT} \tag{2.90}$$

$$= \frac{1}{26\text{ mV}} \quad \text{at } T = 300°\text{K} \tag{2.91}$$

Then solving Eq. (2.89b) for v_{EB}

$$v_{EB} = \frac{1}{K_2}\left[\ln\frac{I_E}{I_{ES}} + \ln\left(1 + \frac{\sqrt{2}\,I_e}{I_E}\cos\omega t\right)\right] \tag{2.92}$$

If the last term in Eq. (2.92) is expanded into a Fourier series, V_{e_1} is determined to be of the form

$$V_{e_1} = \frac{1}{\sqrt{2}\,K_2}\left(\frac{2}{\gamma}\left(1 - \sqrt{1 - \gamma^2}\right)\right) \tag{2.93}$$

where

$$\gamma = \sqrt{2}\,\frac{I_e}{I_E} \tag{2.94}$$

The fundamental transistor input resistance is

$$R_{\text{IN}}(\gamma) = \frac{V_{e_1}}{I_e} = \frac{I_E}{I_e}\frac{V_{e_1}}{I_E} \tag{2.95}$$

$$= \frac{2\left(1 - \sqrt{1 - \gamma^2}\right)}{\gamma^2 K_2 I_E} = \frac{2\left(1 - \sqrt{1 - \gamma^2}\right)}{\gamma^2 g_{m_0}} \tag{2.96}$$

from Eqs. (2.95), (2.93), (2.92), (2.90a), and (2.87).

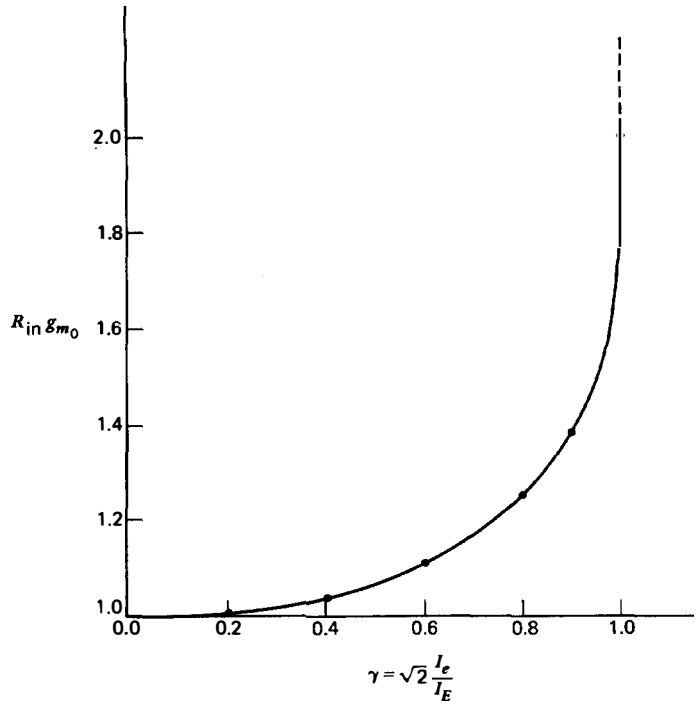

γ	$R_{IN}g_{m_0}$
0.0	1.00
0.1	1.005
0.2	1.01
0.3	1.02
0.4	1.04
0.5	1.07
0.6	1.11
0.7	1.17
0.8	1.25
0.9	1.38
1.0	2.00

Figure 2.15 Normalized input resistance for a sinusoidal emitter current in the common base bipolar transistor.

$R_{IN}(\gamma)g_{m_0}$ as given by Eq. (2.96) is plotted in Fig. 2.15.

It will be noted that the γ axis terminates at $\gamma = 1$, at which point the slope approaches infinity. Equation (2.96) states that, at $\gamma > 1$, $R_{IN}(\gamma)$ becomes complex. This, of course, is true in the ideal model. However, in the real case, this is impossible and, when γ tends to exceed 1, $R_{IN}(\gamma)$ progressively increases at a very rapid but finite rate.

Since i_E cannot be negative, it follows from Eqs. (2.89) and (2.94) that γ cannot exceed 1. Also,

$$I_E \geqq 1.4 I_e \tag{2.97}$$

The latter provides a convenient means of fixing $I_{e_{max}}$.

2.6 BIASING OF BIPOLAR TRANSISTORS

In this section is considered the manner of biasing transistors to yield a given dc emitter current, I_E, from a power source, V_{BB}. The biasing circuit is to produce negligible change in emitter current upon variation of

1 Transistor characteristics.
2 Temperature.
3 Bias shifts due to the ac signals.

Figure 2.16 shows the dc biasing part of an oscillator circuit for a desired I_E. The procedure is as follows:

1 Specify $V_E \geqq 2$ V. (2.98)

2 $r_2 = \dfrac{V_E}{I_E}$ (2.99)

3 Determine the minimum value of β_o.

4 $r_b \approx \dfrac{\beta_o r_2}{5}$ (2.100)

where r_b is the Thévenin source resistance of the dc biasing source and

$$\frac{1}{r_b} = \frac{1}{r_{b_1}} + \frac{1}{r_{b_2}} \tag{2.101}$$

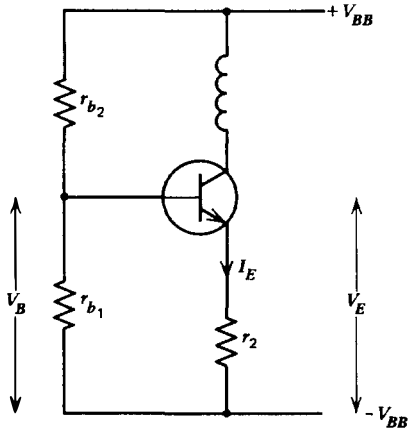

Figure 2.16 dc biasing circuit for the bipolar transistor. *Note*: r_2 is the sum of the bypassed and unbypassed emitter resistors.

5 $V_B \approx V_E + 700\ \text{mV}$ (2.102)
where 700 mV is the average voltage difference between base and emitter for a silicon bipolar transistor.

6 $r_{b_2} = 0.83\frac{V_{BB}}{V_B} r_b$ (2.103)

7 $r_{b_1} = \left(\frac{1}{r_b} - \frac{1}{r_{b_2}}\right)^{-1}$ (2.104)

Equations (2.103) and (2.104) are valid only for $V_B < 0.83V_{BB}$

The following example is investigated:

$V_{BB} = 10$ V
$I_E = 2$ mA
$V_E = 2$ V
β_o min = 20

then

$r_2 = 1000\ \Omega$
$r_b = 4000\ \Omega$
$V_B = 2.7$ V
$r_{b_2} = 12{,}300\ \Omega$, make it 12 k$\Omega$
$r_{b_1} = 5.900\ \Omega$, make it 5.6 kΩ

For the values chosen

$r_b = 3.8$ K
$V_{B_{oc}} = 10\left[\frac{5.6}{12 + 5.6}\right] = 3.18$ V
$V_B = V_{B_{oc}}\frac{20}{20 + 3.8} = 2.67$ V
$V_E = 1.97$ V
$I_E = 1.97$ mA

Let β_o change to 40. Then

$V_B = 3.18\left[\frac{40}{40 + 3.8}\right] = 2.9$ V
$V_e = 2.2$ V
$I_E = 2.2$ mA

so that a 100% change in β_o produces a 10% change in I_E.
Let V_{BE} change to 0.600 V due to temperature and/or ac signal change. For

the original transistor ($\beta_o = 20$)

$V_B = 2.67$ V
$V_E = 2.07$ V
$I_E = 2.07$ mA

so that a 100-mV change in V_{BE}, which is quite large, produces a 3% change in I_E.

2.7 THE JUNCTION FIELD EFFECT TRANSISTOR

2.7.1 Introduction

A brief presentation of the properties of the junction field effect transistor (JFET) is now made, as some of the important properties are considerably different from those of the bipolar transistor. The major differences are summarized in Table 2.3 for the common emitter/source connection at low and medium frequencies for high-performance transistors.

In addition, it should be noted that the bipolar transistor requires only knowledge of the β_o, f_T, and the power dissipation rating to be almost completely specified, while the JFET requires knowledge of many more parameters.

As shown in Table 2.3, the g_m of the JFET is much smaller than that of the bipolar transistor. Therefore, the JFET will be used primarily in those applications where the very high input impedance of the JFET is advantageous. This is true for crystals having very high resistances such as those at low frequencies.

Another important property of the JFET is its relatively low noise, as discussed in Chapter 14.

2.7.2 Ideal Small-Signal Relationships in JFETs at Low and Medium Frequencies

1 Variation of drain current with gate bias

$$I_D = I_{DSS}\, 1 - \left(\frac{V_{GS}}{V_{GS(\text{off})}}\right)^2 \tag{2.105}$$

where I_{DSS} is the current at $V_{GS} = 0$ (2.106)

$V_{GS(\text{off})}$ is the voltage at $I_D = 1\ nA$ (2.107)

Table 2.3 Comparison of Bipolar and JFET Transistors

Parameter or Characteristic	Bipolar at Large V_{CE}	JFET in Pinch-Off Region	Typical value at $I_{C/D} = 5$ mA	
			Bipolar	JFET
Ideal relationship $i_{C/D}$ versus $v_{BE/GS}$	Exponential	Square law		
Small-signal g_i	Large, proportional to I_C	Very small, weak function of I_D	2 m℧	< 0.001 m℧
Small-signal $g_f = g_{m_0}$	Large, proportional to I_C	Small, proportional to I_D	200 m℧	5 m℧
Small-signal C_i	Proportional to I_C	Weak function of I_D	35 pF	4 pF

2 Variation of g_{fs} with V_{GS}

$$\left(g_{m_0} \equiv g_{fs}\right) = g_{fs0}\left(1 - \frac{V_{GS}}{V_{GS(\text{off})}}\right) \tag{2.108}$$

where

$$g_{fs0} \text{ is } g_{fs} \text{ at } V_{GS} = 0 \tag{2.108a}$$

3 Variation of g_{fs} with I_D

$$g_{m_0} \equiv g_{fs} = g_{fs0}\sqrt{\frac{I_D}{I_{DSS}}} \tag{2.109}$$

4 Relationship for g_{fs0}

$$g_{fs0} = \frac{2I_{DSS}}{V_{GS(\text{off})}} \tag{2.110}$$

5 Relationship between I_{DSS} and $V_{GS(\text{off})}$ for a given transistor type:

$$I_{DSS} \propto V_{GS(\text{off})} \tag{2.111}$$

Thus, when $V_{GS(\text{off})}$ increases, I_{DSS} also increases.

The above relationships demonstrate the great importance of I_{DSS} and $V_{GS(\text{off})}$, which vary widely. It is therefore, at present, impractical to develop useful universal models similar to those for the bipolar transistor.

2.7.3 Small-Signal High-Frequency Characteristics

Figure 2.17 shows the y parameters versus frequency characteristics for the 2N4416A which is a very popular high-performance JFET. All these parameters are at $I_D = I_{DSS}$ which is an unusually large current.

Study of this figure discloses the following:

1 $g_{is} \approx 2.5(10)^{-5} f^3\ \mu\mho$
   f in MHz
2 $b_{is} \approx 10f\ \mu\mho$ which is equivalent to a capacitance of 1.5 pF.
3 g_{os} is flat to 100 MHz at about 0.05 m$\mho$ and decreases with I_{DSS}.
4 $b_{os} \approx 5f\ \mu\mho$ which is equivalent to about 0.9 pF.
5 $g_{fs} \approx 5\ \mho$ until about 400 MHz.
6 $b_{fs} \approx 10f\ \mu\mho$

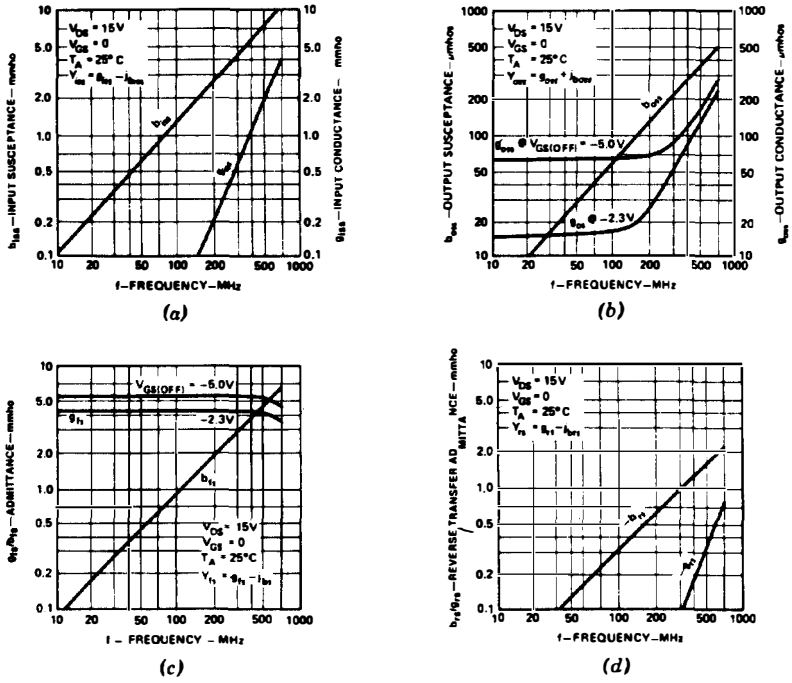

Figure 2.17 y parameters versus frequency for the 2N4416A common source junction FET. (*a*) y_{is}. (*b*) y_{os}. (*c*) y_{fs}. (*d*) y_{rs}. (Courtesy of Teledyne Semiconductor.)

7 Items 5 and 6 imply that

$$\theta_{y_{fs}} \approx (0.12f)^\circ$$

8 $b_{rs} \approx 3f\ \mu\mho$ which is equivalent to about 0.45 pF.

9 Items 4 and 8 imply that

$$C_{dg} \approx C_{ds} \approx 0.45 \text{ pF}$$

It cannot be too highly stressed that the above values are subject to extremely wide variations due to the manufacturing process, but they give the orders of magnitude to be expected.

2.7.4 JFET Common Source Large-Signal Characteristics

As indicated in Table 2.3, the relationship between I_D and V_{GS} is square law. As a result, the large-signal characteristics, described in Section 2.4, which form the basis for one desirable type of limiting, are not applicable for the JFET. However, the very high input impedance of the JFET makes possible

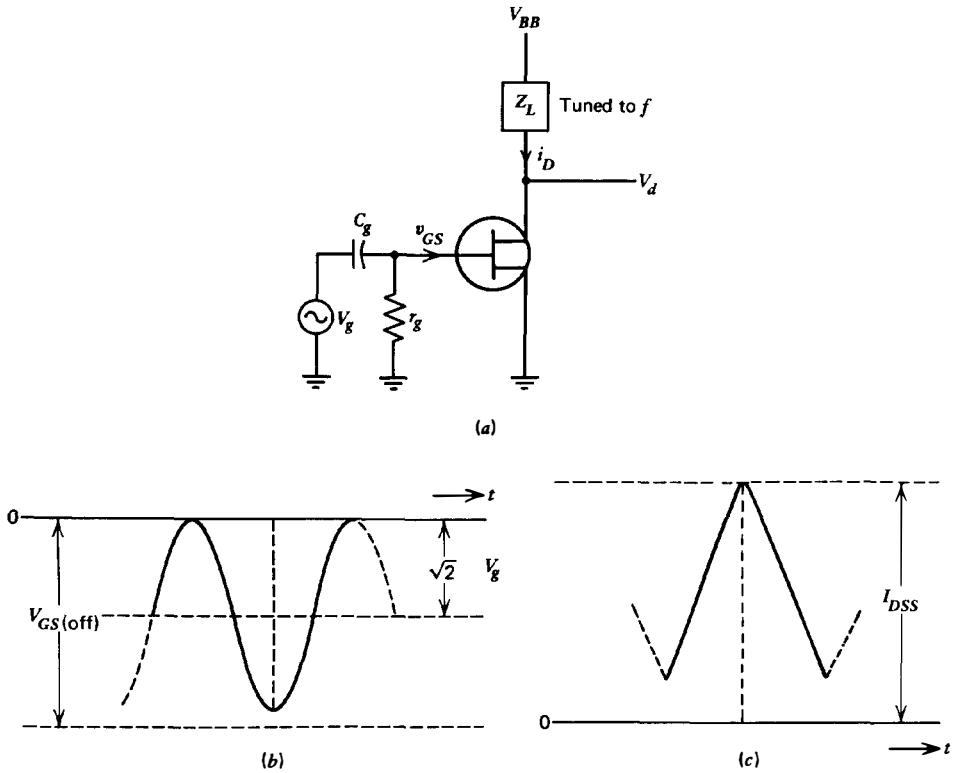

Figure 2.18 The JFET clamp biased amplifier. (*a*) Circuit diagram. (*b*) Wave shape of v_{GS}. (*c*) Wave shape of i_D.

the useful large-signal circuit, known as the clamp biased amplifier and described below. The treatment is based upon the procedure beginning on page 131 of Ref. 2.3,† and will present essentially only the final results. Those interested in more detail may consult the reference.

The Clamp Biased Amplifier Circuit

Consider the circuit shown in Fig. 2.18*a*. Clearly, in this circuit, if the r_gC_g time constant is much greater than $T = 1/f$, the capacitor voltage charges to the peak value of v_G and remains constant at that value; hence

$$v_{GS} = \sqrt{2}\, V_g[\cos(2\pi ft) - 1] \tag{2.112}$$

The input voltage, v_{GS}, to the transistor is thus clamped to zero and has the

†Clarke/Hess, *Communication Circuits: Analysis and Design*, © 1971, Addison Wesley, Reading, Mass., Fig. 4.9-4 (modified). Reprinted with permission.

wave shape shown in Fig. 2.18*b*. The drain current i_D has the wave shape shown in Fig. 2.18*c* due to the square-law characteristics as given by Eq. (2.105). When $\sqrt{2}\,V_g = V_{GS(\text{off})}$, the width of the i_D pulse is 360°. However, when $\sqrt{2}\,V_g > V_{GS(\text{off})}$, the width decreases as V_g increases. The load, since it is tuned to f, will respond only to the fundamental component I_d of i_D.

Let

$$g_m = \frac{I_d}{V_g} \tag{2.113}$$

and

$$\alpha = \frac{g_m}{g_{m_0}} \tag{2.114}$$

where g_{m_0} is given by Eq. (2.110).

If a Fourier analysis is made of the i_D characteristics to obtain I_d as a function of V_g and α computed as a function of $V_g/-V_{GS(\text{off})}$ and plotted, Fig. 2.19 results.

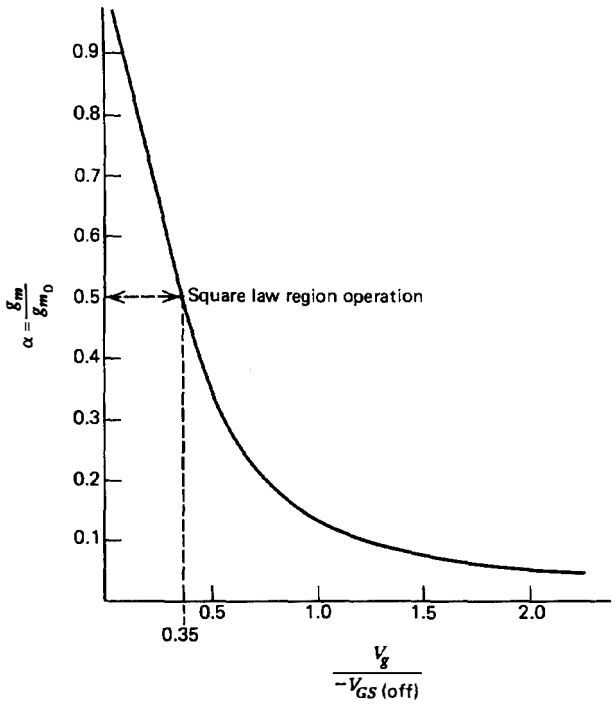

Figure 2.19 Plot of α versus $V_g/-V_{GS(\text{off})}$.

Table 2.4 Values of I_d / I_{DSS} and I_D / I_{DSS}

$\frac{V_g}{-V_{GS(off)}}$	$\frac{I_d}{I_{DSS}}$	$\frac{I_D}{I_{DSS}}$
0	0	1
0.35	0.35	0.37
0.5	0.33	0.30
1.0	0.27	0.20

Additional Fourier analysis will produce curves for I_d/I_{DSS} and I_D/I_{DSS}. These curves are not shown, but some useful points are given in Table 2.4.

Another useful relationship is

$$r_{g_{ac}} = \frac{r_g}{3} \tag{2.115}$$

It should be noted that all the material in this section is valid only when

$$v_{D\,\min} < v_{G\,\max} \tag{2.116}$$